Characterization of soil surface properties using radar remote sensing

Nicolas Baghdadi

scholar.google.com/citations?user=tgPf6rUAAAAJ
https://www.researchgate.net/profile/Nicolas_Baghdadi/?ev=hdr_xprf

June 2022

➢ **Nicolas BAGHDADI**

- Research Director, INRAE (French National Research Institute for Agriculture, Food and Environment), France
- Scientific Director of the French Land Data center Theia
- Associate Editor for the Remote Sensing Journal

nicolas.baghdadi@teledetection.fr

➢ Main field of interest: analysis of remote sensing data (mainly radar and lidar) and the retrieval of environmental parameters (e.g. soil moisture content, soil roughness, canopy height, forest biomass …).

➢ Main research topics:

✓ Soil parameters estimation from SAR data over bare agricultural fields
✓ Forest height and aboveground biomass estimation from ICESat/GLAS lidar data
✓ SAR data and wetlands mapping
✓ Potentiel of SAR for monitoring sugarcane crops
✓ Potential of SAR data for mudbank monitoring
✓ Surface and subsurface structural mapping using low frequency radar
✓ Potential of radar images for wet snow mapping
✓ …

Objective

➢ The objective of this course is to present:

(1) the behavior of the C-band radar signal as a function of soil parameters of agricultural plots (mainly moisture and roughness)

(2) approaches to mapping moisture and roughness by coupling radar et optical images

Plan

1. Describe the instrumental parameters of radar sensors that influence the backscattered signal
2. Describe the soil parameters, in particular roughness and moisture
   - 2.1 Roughness
   - 2.2 Soil moisture
3. Behavior of the radar signal
   - 3.1 Penetration depth of the radar wave
   - 3.2 Sensitivity of the radar signal to ground parameters
     - 3.2.1 Sensitivity of the radar signal to roughness
     - 3.2.2 Sensitivity of the radar signal to moisture
     - 3.2.3 Sensitivity of the radar signal to salinity
     - 3.2.4 Sensitivity of the radar signal to soil freezing
4. Modeling the radar signal
   - 4.1 Case of bare soil
   - 4.2 Case of soils with vegetation
5. Estimation of soil moisture

1. Instrumental parameters of radar sensors

SAR systems

- SAR stands for Synthetic Aperture Radar (SAR)

- Active system: provides its own source of electromagnetic energy ➔ Images day and night, with or without clouds

- ERS-1/2 (EU): first global and regular coverage SAR sensors, early 90s: 35-day repeatability, formerly paid data

- Since 2016, Sentinel-1A/1B provides an image every 6 days, open and free data ➔ Data adapted to agronomic and hydrological applications at local or regional scales (10 m pixel)

- A response to local and global issues:
  - Territorial development
  - Manage the environment
  - Understand the effects of climate change / anthropogenic pressure

Remote sensing process

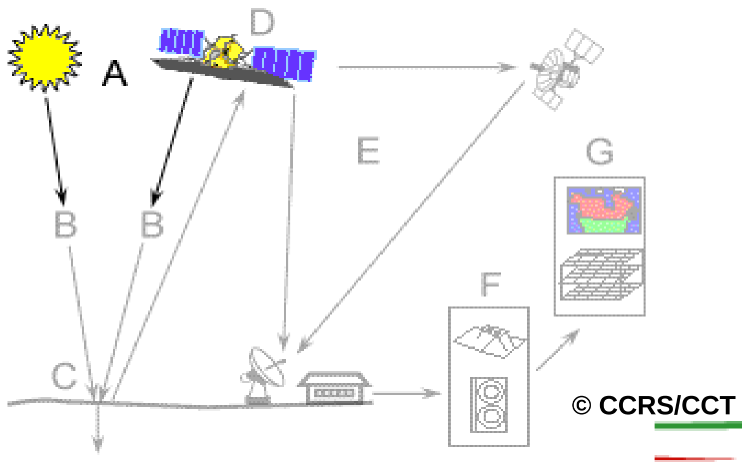

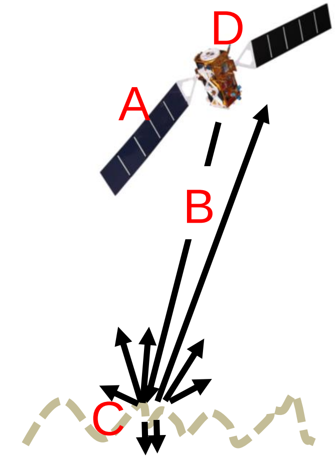

A: Illumination, **Sun for optical sensors, Antenna for radar sensors**

B: Interaction between the radiation and the atmosphere

C: Interaction with the target

D: Recording of backscatterd energy by the sensor

E: Transmission

F: Interpretation and analysis

G: Applications

➔ Spatial remote sensing is of vital importance for the mapping and monitoring of environmental problems: global and permanent information

Instrumental parameters

- Three major instrumental parameters: wavelength, polarization and incidence angle.

- SAR sensors currently operational: TerraSAR-X, Cosmo-SkyMed, Sentinel-1, RADARSAT-2, ALOS/PALSAR-2 …

- SAR Archive: ERS, ASAR/Envisat, RADARSAT-1, PALSAR/ALOS …

- The radar signal depends on:

➢ characteristics of the wave emitted (wavelength, incidence and polarization)

➢ characteristics of the environment. In the case of soil without vegetation roughness, soil moisture, soil composition…

Instrumental parameters

- Radar wavelength (λ) = length of a cycle of a wave

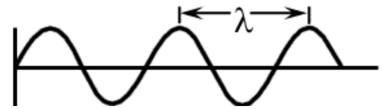

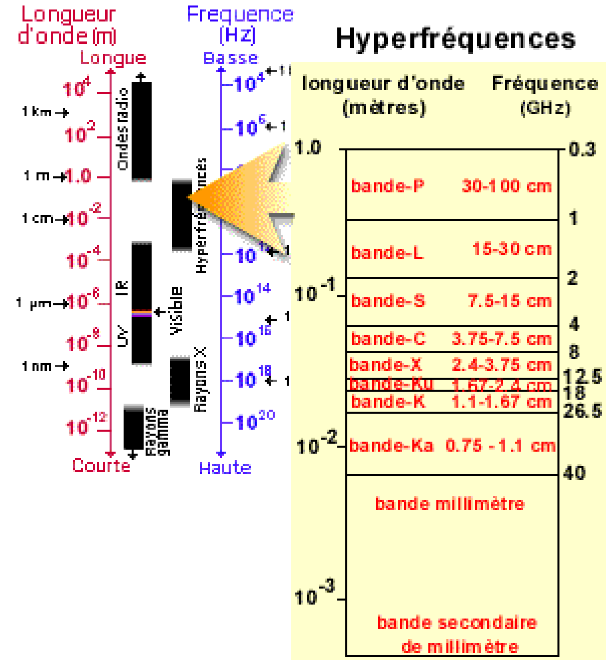

Sentinel-1: λ~5.6 cm

- Incidence angle (θ): the angle measured between the radar beam and the normal

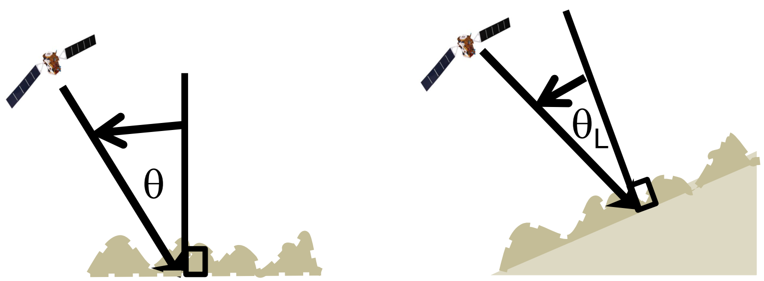

- Polarization: Orientation of the electric field of the electromagnetic wave. Linear polarizations ➔ HH, VV, HV and VH

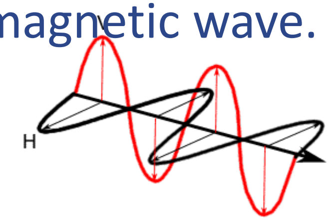

Current SAR sensors

- There are currently many radar sensors in operation: RADARSAT-2, TerraSAR, CosmoSkyMed, PALSAR-2/ALOS and Sentinel-1

- The only one that provides free and open access data is Sentinel-1

- Sentinel-1 (S1): European sensor, C band (λ~6 cm), spatial resolution = 10 m, two satellites 1A and 1B

- A temporal resolution better than the week

- Image download:

1- Sentinel-1 hub : https://scihub.copernicus.eu/dhus/#/home

2- Peps: https://peps.cnes.fr/rocket/#/home

…

- Processing of S1 images: https://sentinel.esa.int/web/sentinel/toolboxes

Sentinel-1

PRODUITS IMAGES

Sentinelle 1

Mode d'imagerie	Radar
Bandes spectrales	Bande C (~ 6 cm de longueur d'onde)
Incidence	18 ° - 47 °
Polarisation	HH, VV, HH+HV, VV+VH
Résolution spatiale	10 m
Capacité d'observation	Fauchée : 250 km Répétitivité : 12 jours (1 satellite) / 6 jours (2 satellites)
Couverture systématique	Zone : monde Période : 2015 - présent
Produits	Brut
Accès	Tous utilisateurs sur scihub.esa.int Tous utilisateurs sur peps.cnes.fr

Exemple

Image radar Sentinelle 1A de l'agglomération de Lisbonne (Portugal) © Copernicus data/ESA (2014)

Soil applications

- Soil moisture and surface roughness play an important role in many applications

- Surface runoff occurs when rainfall intensity exceeds the soil infiltration capacity. In addition to vegetation, soil roughness also plays a role of trapping water in agricultural areas, which increases infiltration and in turn reduces downstream runoff.

- Bare soils are most implicated in the considerable risk of runoff and erosion in agricultural areas.

2. Soil parameters: surface roughness et soil moisture

Definition, in situ measurements

2.1 Soil roughness

Description of soil roughness

- ***Description of soil roughness***
  - Several techniques can be used to measure soil roughness: pin profilometer, laser profilometer, and 3D photogrammetry.
  - The use of the laser or 3D photogrammetry allows for the accurate rendering of soil roughness (high spatial resolution) with a precise estimation of the roughness parameters, *Hrms* and *L*.
  - As regards the correct characterization of soil roughness using a pin profilometer, it is necessary to have (1) long roughness profiles or several short profiles and (2) a relatively fine horizontal resolution from the profilometer (small sampling interval, Δx).

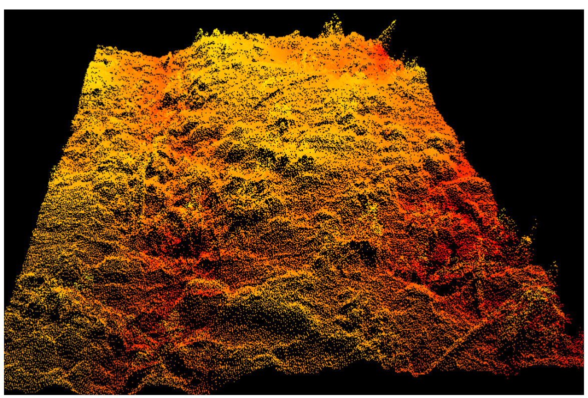

2D profile from a laser scanner

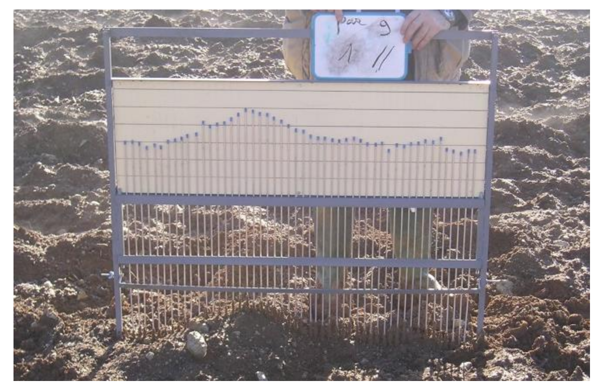

1D profile from a pin profilometer (1 m long and Δx = 2 cm)

- ***Description of soil roughness***
  - For SAR applications, the description of the surface z(x) is based on the calculation of the autocorrelation function ρ(u), defined as: (1D case)

$$\rho(u) = < [z(x+u)-<z>]\,[z(x)-<z>] >$$

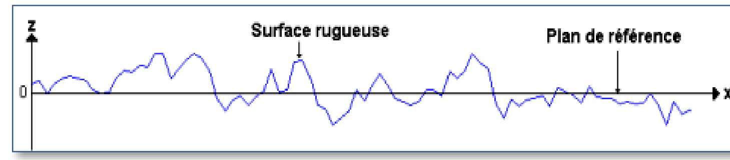

$\langle z \rangle$ is the average height of altitudes measured from the roughness profile z(x).

  - Generally, two roughness parameters are used and estimated based on the autocorrelation function:
    - The standard deviation of the surface height (root mean square surface height, Hrms), defining the vertical scale of the roughness and computed as:

$$Hrms^2 = \rho(0) = < [z(x)-<z>]^2 >$$

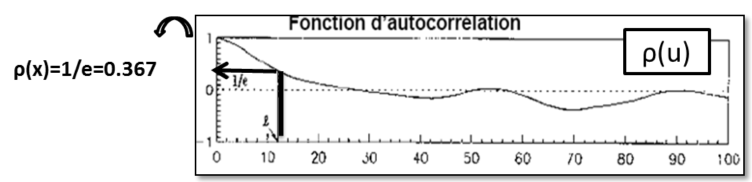

    - The correlation length (*L*), usually defined as the horizontal displacement for which the autocorrelation function of the profile decreases to 1/e.

Description of soil roughness

- ***Description of soil roughness***
  - When the roughness is weak and the soil is smooth (*Hrms* approximately inferior to 1 cm), the autocorrelation function has a generally exponential shape.
  - For higher roughness, the autocorrelation function has a shape close to a Gaussian.
  - Zribi [ZRI 98] introduced the fractal dimension to the description of the autocorrelation function's shape for bare soils in agricultural fields. For one-dimensional roughness profiles:

$$\begin{aligned}
\rho(x) &= Hrms^2\, e^{-\left(\frac{x}{L}\right)} && : \quad \text{exponential} \\
&= Hrms^2\, e^{-\left(\frac{x}{L}\right)^2} && : \quad \text{Gaussian} \\
&= Hrms^2\, \mathrm{e}^{-\left(\frac{\mathrm{x}}{\mathrm{L}}\right)^{\alpha}} && : \quad \text{fractal}
\end{aligned}$$

α = -2D+4, *D* is the fractal dimension between 1.25 and 1.45 ➔ autocorrelation function power a between 1.1 and 1.5.

Description of soil roughness

- ***Description of soil roughness***
  - In the case of agricultural surfaces with periodic structures (rows, with *P* periods), the autocorrelation function could be described by (in the case of a Gaussian shape, for example):

$$\rho(x) = Hrms^2 e^{-\left(\frac{x}{L}\right)^2} + S^2 e^{-\left(\frac{x}{L_S}\right)^2} \cos\left(\frac{2\pi x}{P}\right)$$

  - The second term models the directional roughness variations as a narrowband Gaussian random process, centered on a frequency ($1/P$) and a band length of $2\pi/L_S$. A Fourier transform of this term allows the deduction of the 3 parameters describing the directional structure (the intensity *S*, the periodicity *P*, and the correlation length L_S).

2.2 Soil moisture

- ***Description of soil moisture***
  - There are two commonly used techniques for the measurement of soil moisture content: gravimetry and Time-Domain Reflectrometry (TDR) (or Theta Probe analysis).
  - The gravimetric method, while destructive and complicated to implement, remains a reference for the calibration of different equipment used to measure soil moisture.
  - The gravimetric method consists in using a cylinder to collect soil samples, which are then placed in an oven at 105ºC for 24h. This method determines the ponderal water content (*Wp*) of a soil sample by comparing the wet weight (*Ph*) of the sample with its dry weight (*Ps*):

$$Wp\ (g.g^{-1}) = 100\left(\frac{Ph - Ps}{Ps}\right)$$

  - The volumetric water content *mv* (in $cm^3.cm^{-3}$ or vol. %) is deduced from the ponderal water content using the soil's apparent density (*Da=Ps* / volume of the cylinder):

$$mv = Da\,.Wp$$

Soil moisture

- ***Description of soil moisture***
  - The TDR probe consists in emitting an electromagnetic microwave pulse along 2 (sometimes 3) waveguides of a given length, inserted into the soil, and measuring the transit time of the return signal.

  - TDR measurements are not valid for frozen soils
  - In-situ soil moisture data is generally collected simultaneously with radar acquisitions.
  - The distribution and spatial density of these measurements depend upon the level of heterogeneity of reference plots (intra-plots variations) and their size. A minimum of 20 measurements is generally taken for each reference plot (measuring at least one hectare).

- ***Description of soil moisture***
  - Bruckler et al. [BRU 88] found that the penetration depth of the radar signal in C-band for a clay loam soil decreases from 5 to 1 cm when the soil moisture increases from 10 to 30 vol. % .
  - The dielectric constant is a physical quantity also known as complex permittivity. The real part ε' affects the moisture content more, while the imaginary part ε" essentially depends on the electrical conductivity of the soil solution.
  - The empirical relationship between the volumetric water content of soil and its dielectric constant described by Topp et al. [TOP 80] is also widely used for its simplicity. This relation only allows the derivation of the real component of the dielectric constant:

$$mv = (-530 + 292\,\varepsilon - 5.5\,\varepsilon^2 + 0.043\,\varepsilon^3).10^{-4}$$

3. Behaviour of radar signal

3.1 Penetration depth of radar wave

Penetration of radar wave

- When performing studies using radar images in L, C, and X bands for the characterization of the soil surface moisture in agricultural areas, in-situ measurements of soil moisture are taken at a depth between 0 and 10 cm.
- The measurement depth is related to the penetration depth of the radar wave (δ_p) that is generally equal to a few centimeters in C and X bands. In L-band, this depth can reach a few tens of cm for very dry soils.
- The thickness of this surface layer depends on the radar wavelength (λ) (more penetration with greater wavelengths) and the dielectric constant of soil (water content and soil composition) [ULA 78]:

$$\delta_p \cong \frac{\lambda\sqrt{\varepsilon'}}{2\pi\sqrt{\varepsilon''}}$$

ε' is the real part of the dielectric constant and ε'' its imaginary part.

- Longer λ (P and L bands) can penetrate deeper than shorter λ (C and X bands)

Relationship between moisture and dielectric constant

- Relationship between soil volumetric water content (mv) and its dielectric constant from Topp et al. (1980). It allows the calculation of the real component of the dielectric constant (ε'):

$$mv = (-530 + 292\,\varepsilon' - 5.5\,\varepsilon'^2 + 0.043\,\varepsilon'^3).10^{-4}$$

- A more detailed relationship proposed by Hallikainen et al. (1985):

$$\varepsilon = \varepsilon' - j.\,\varepsilon''$$

$\varepsilon' = [a_{0r} + a_{1r}\,.\,sand + a_{2r}\,.\,clay]$	$\varepsilon'' = [a_{0i} + a_{1i}\,.\,sand + a_{2i}\,.\,clay]$
$+[b_{0r} + b_{1r}\,.\,sand + b_{2r}\,.\,clay].mv$	$+ [b_{0i} + b_{1i}\,.\,sand + b_{2i}\,.\,clay].mv$
$+ [c_{0r} + c_{1r}\,.\,sand + c_{2r}\,.\,clay].mv^2$	$+ [c_{0i} + c_{1i}\,.\,sand + c_{2i}\,.\,clay].mv^2$

✓ The coefficients a_{0r}, a_{1r}, … , c_{2i} depend on radar frequency

✓ Sand = percent of sand in the soil ; Clay = percent of Clay in the soil

Penetration of radar wave

- **From Hallikainen et al. (1985):**
  - Field 1: 52% sand, 13% clay, 35% Silt
  - Field 5: 5% sand, 47% clay, 48% Silt

- **Observations:**
  - ✓ ε' et ε'' increase when *mv* increases
  - ✓ ε' higher for soils with more sand ➔ δ_p higher
  - ✓ ε'' lower for soils with more sand only if the soil is very wet // otherwise ε'' changes slightly if *mv* <20 vol.%

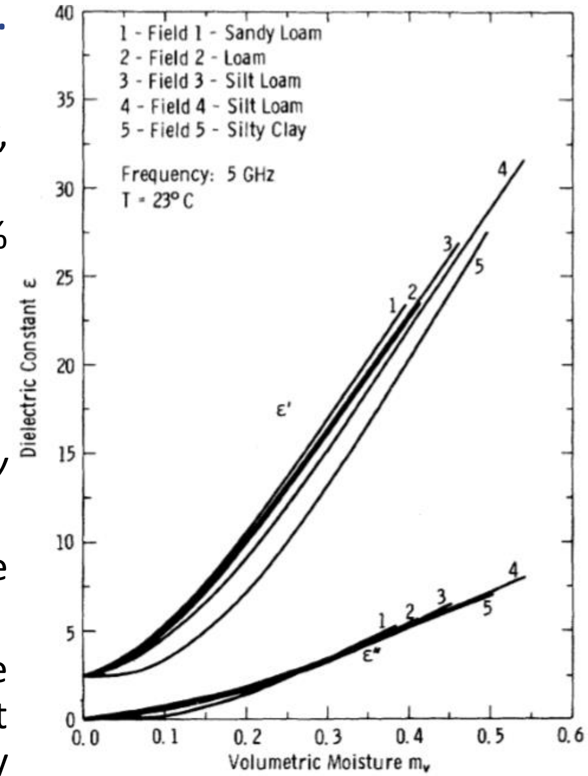

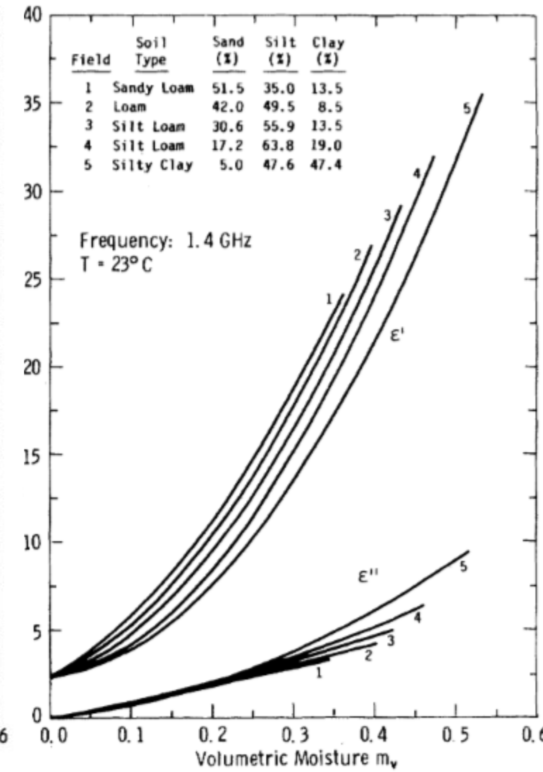

For radar frequency = 5 GHz (λ=6 cm) and mv=20 vol.%	For radar frequency = 1.4 GHz (λ=21 cm) and mv=20 vol.%
Field 1: ε' = 11 et ε'' = 2 ➔ δp= 2.2 cm	Field 1: ε' = 10 et ε'' = 2.5 ➔ δp= 7 cm
Field 5: ε' = 7 et ε''= 2 ➔ δp= 1.8 cm	Field 5: ε' = 7 et ε''= 2.5 ➔ δp= 6 cm
➔ More penetration in the sand	➔ More penetration for high λ

Penetration in arid areas

- Since the penetration depth of the radar wave is proportional to the radar wavelength, it is possible in desert region using long wavelengths to highlight hydrographic networks covered by a layer of sand (of several m) and which are invisible on optical images.

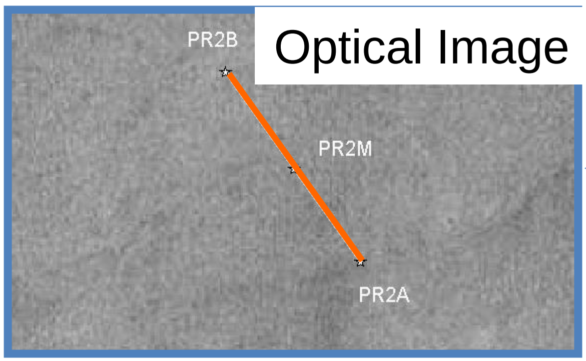

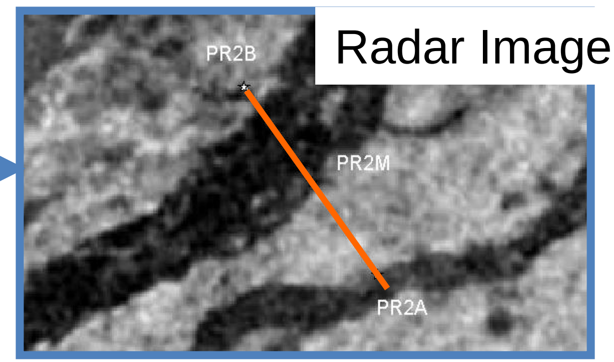

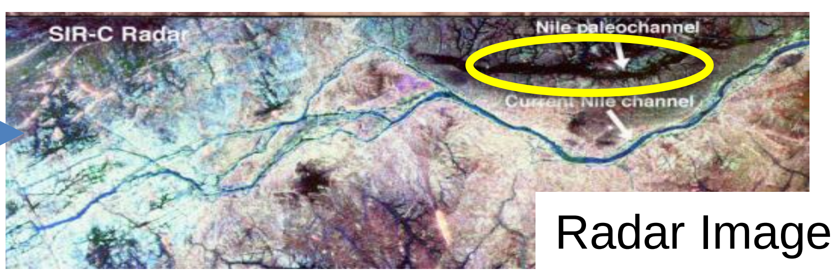

3.2 Sensitivity of radar signal to soil parameters

Approach for mapping soil parameters

✓ Remote Sensing

« Radar »

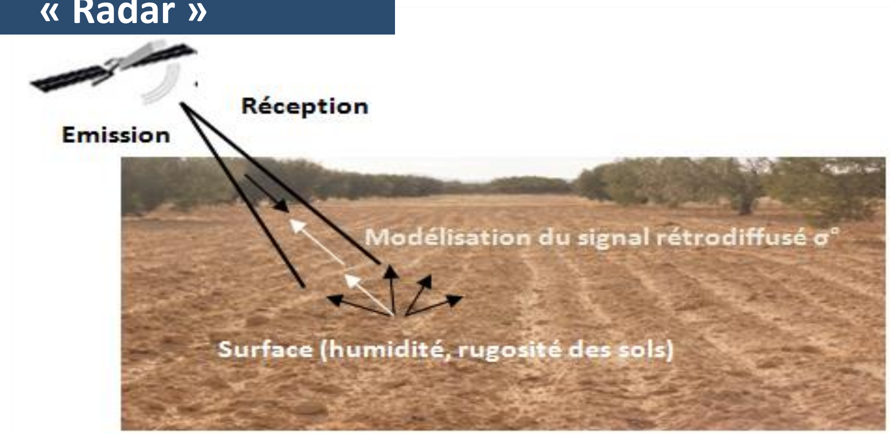

MODELLING RADAR BACKSCATTERING

- **Radar observation parameters:**
(frequency , incidence angle,…)
- **Soil surface parameters:**
(**soil moisture,** roughness..)

Electromagnetic backscattering Models (Kirchoff, Dubois, Oh, Integral Equation Model …)

Radar Backscatter σ^0

RADAR SIGNAL INVERSION

Practical instructions (1/2)

- Perform a bibliographic analysis to identify, for example, the optimal instrumental parameters capable of mapping (1) roughness, (2) soil moisture, etc.

- Choose control agricultural plots on which roughness and moisture measurements are taken → in situ measurements

- Create a vector file with control plots or "AOI: Area Of Interest“

- Processing radar images: radiometric calibration, georeferencing

- Warning: Select control plots of 100 radar pixels and more to have relevant statistics (minimize the speckle effect / noise effect)

Practical instructions (2/2)

- Calculate statistics using the vector file or AOIs: average radar signal

  - The images calibrated in linear scale must be used for the calculation of the average radar signal on a given plot or an AOI

  - Once the average radar signal has been calculated (in linear scale), the signal is calculated in decibel (dB) scale using the formula:

$$\sigma^\circ \text{ in dB} = 10 \,.\, \log10\,(\sigma^\circ \text{ in linear scale})$$

- Analyze signal behavior based on sensor and ground parameters

- Model the radar signal or validate existing models

- Extract useful information by inverting the radar signal (surface roughness/moisture, etc.)

3.2.1 Sensitivity of radar signal to roughness

Interest of soil roughness

- Soil roughness plays an important role in the runoff/infiltration ratio.

- Runoff occurs when the intensity of precipitation exceeds the infiltration capacity of the soil.

- In addition to vegetation, soil roughness also plays a role in trapping water in agricultural areas, which increases infiltration and in turn reduces downstream runoff.

- In agricultural areas, bare soils are most implicated in the risk of runoff and erosion.

- Watershed-scale monitoring tools are needed to improve flood prediction ➔ monitoring of surfaces that may contribute runoff.

An application example : Excess runoff and remote sensing

Interest of soil roughness

➢ **Smooth soils have commonly a poor infiltration capacity compared to rough soils**

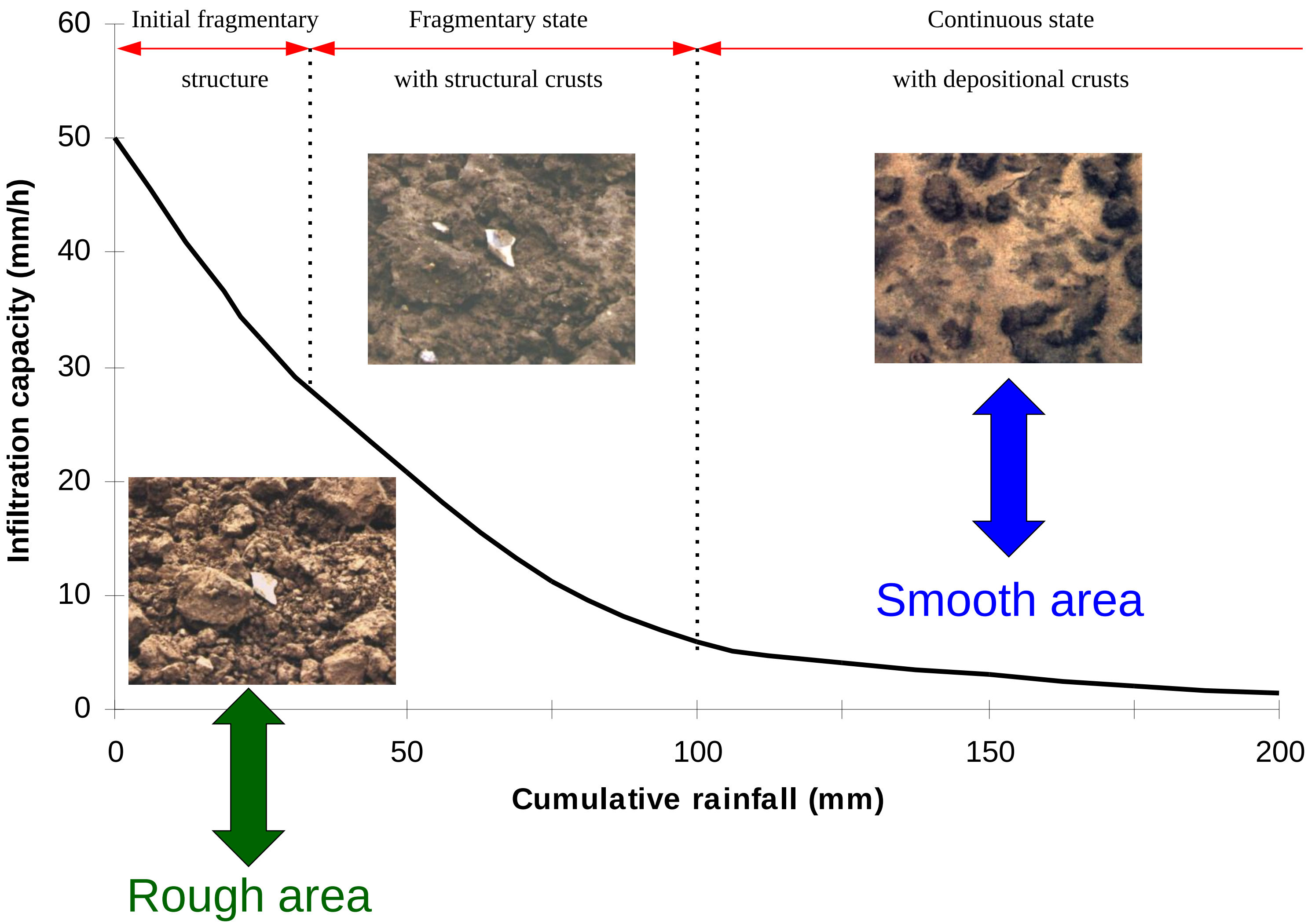

Radar signal and soil roughness

- Smooth surfaces : reflect almost all incident energy away from the radar, are called specular reflectors. They appear dark on radar images (calm water, etc.) ➔ weak radar signal

- Rough surfaces : scatter incident microwave energy in many directions (diffuse reflection). They therefore appear as clear areas on the radar images ➔ strong radar signal

- For a given λ, a surface appears smoother as θ increases.

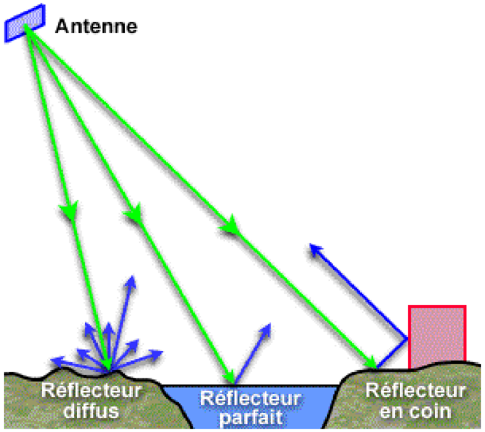

Radar signal and soil roughness

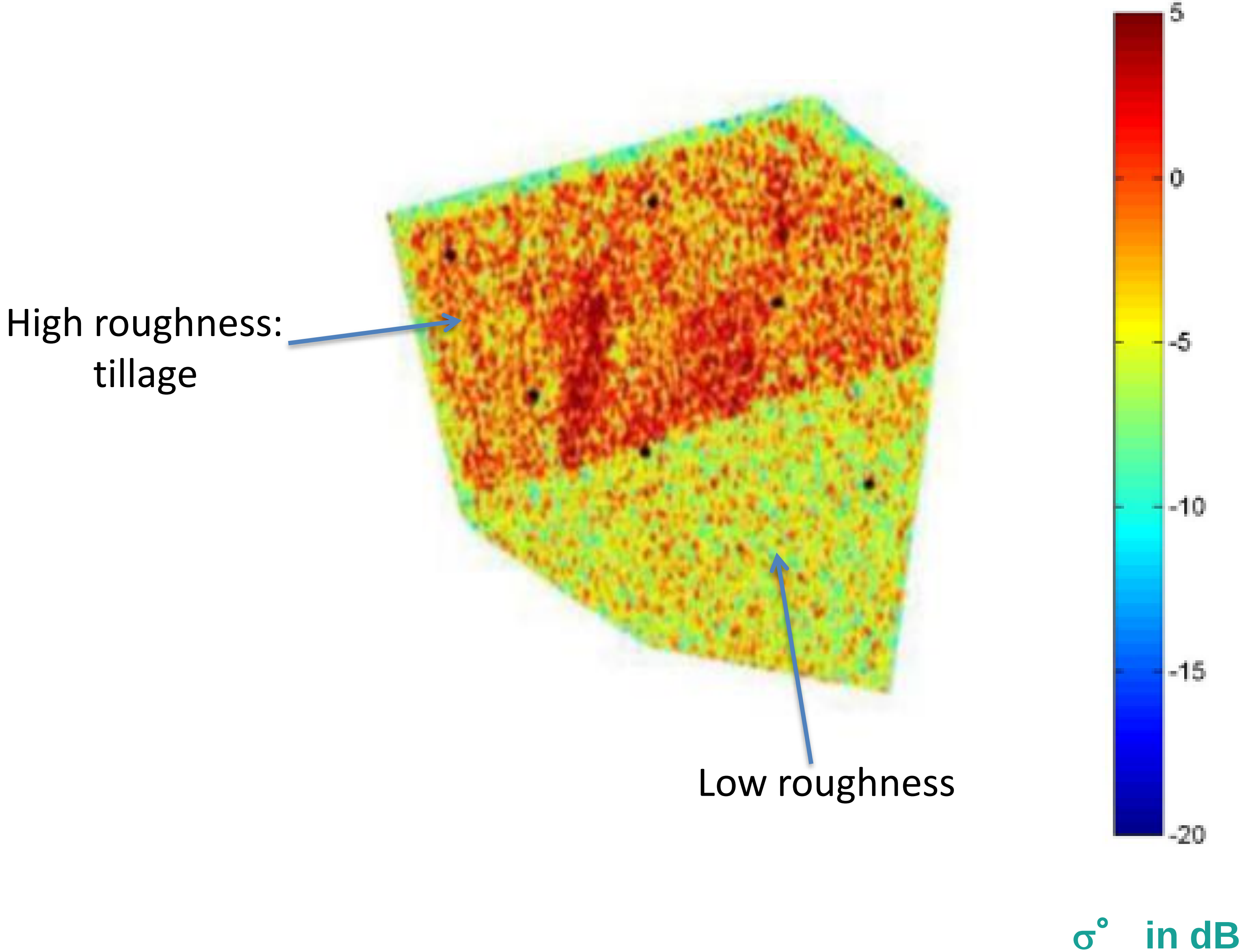

Sensitivity of radar signal to soil roughness

Each point corresponds to the average radar signal and the associated roughness measurement (N averaged measurements)

$\sigma°$ Low incidence ~ 20°

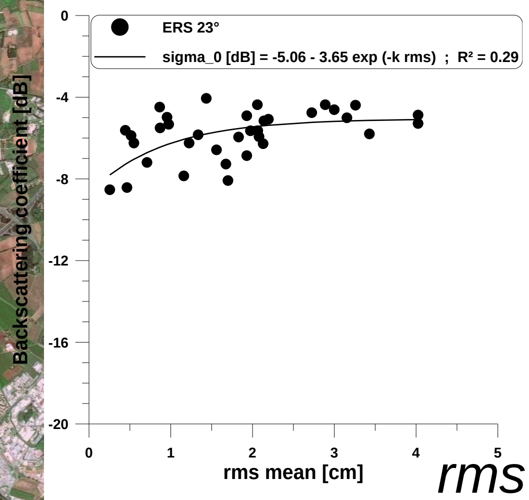

$\sigma°$ Middle incidence ~ 40°

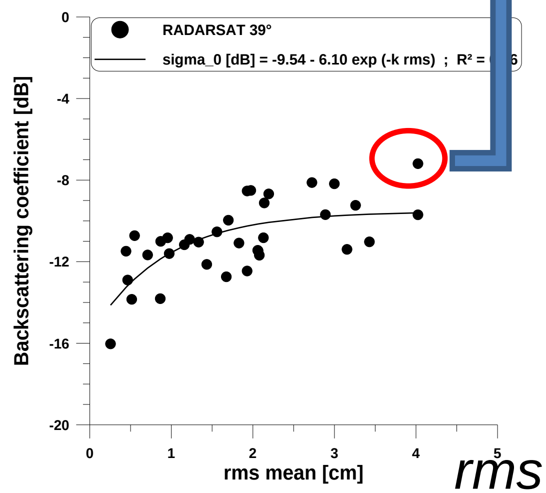

$\sigma°$ High incidence ~50°

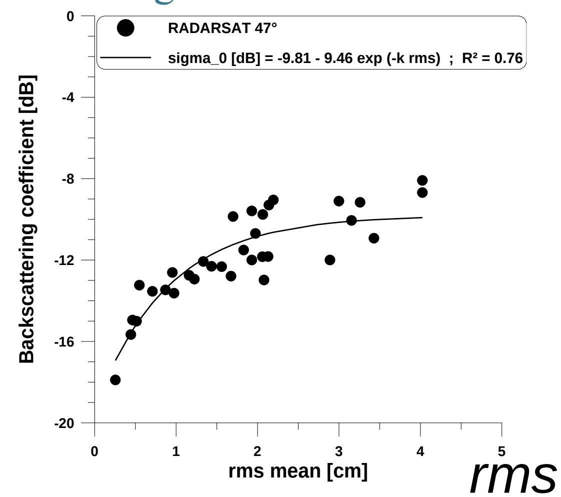

Behavior of radar signal as a function of surface roughness (rms)

- For bare soils, $\sigma°$ increases and follows exponential function with *rms*.
- Extraction of surface roughness is better at high incidence angle: a good indicator for monitoring surfaces potentially contributing to runoff.
- Dependence of radar signal on surface roughness in agricultural areas is mainly significant for low levels of roughness.

Sensitivity of radar signal to soil roughness

- To analyze the sensitivity of the radar signal to soil roughness according to radar wavelength (λ), $\sigma°$ is ploted according to *k.Hrms* with *k* = wave number= $(2\pi)/\lambda$

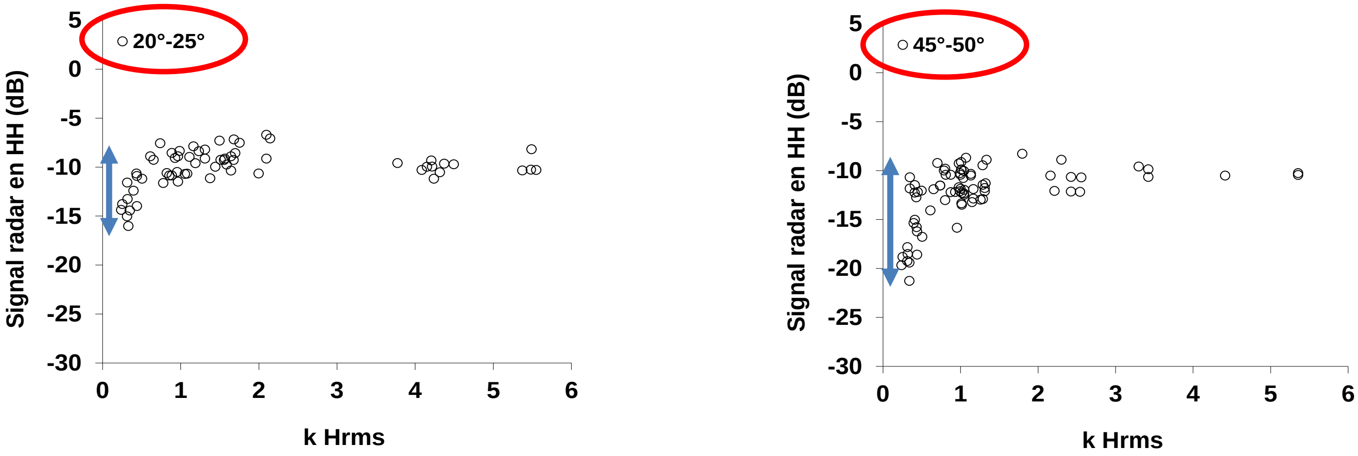

- We observe a sensitivity of $\sigma°$ to *k.Hrms* only for *k.Hrms* < 1:

- In X-band: it corresponds to *Hrms* < 0.5 cm
- In C-band: it corresponds to *Hrms* < 1 cm
- In L-band: it corresponds to *Hrms*< 4 cm

Bande X	Bande C	Bande L
λ = 3 cm	λ = 6 cm	λ = 25 cm
$k \sim 2$ cm^{-1}	$k \sim 1$ cm^{-1}	$k \sim 0{,}24$ cm^{-1}

→ Better sensitivity of $\sigma°$ to *Hrms* for sensors at high λ

Sensitivity of radar signal to soil roughness

- The best sensitivity of the signal to Hrms is observed at high incidences
- Theoretical and experimental work shows a slightly higher sensitivity of the signal to the roughness of bare soils in HH polarization
- The radar signal increases with Hrms according to an exponential/logarithmic law up to a certain threshold

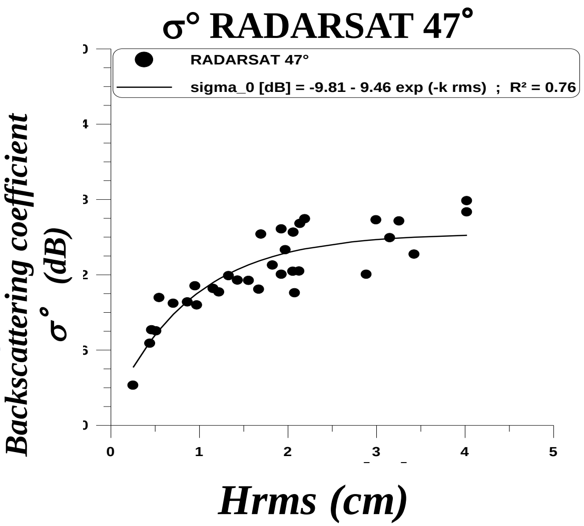

- The sensitivity of $\sigma°$ to *Hrms is* significant for low *Hrms: at* 47°, $\sigma°$ increases of 5 dB (-18 ➔ -13 dB) when *Hrms* increases from 0.25 to 1 cm. It increases only of 1 dB (-11 ➔ -10 dB) when *Hrms* increases from 2 to 4 cm

- Possibility of extracting 2-3 classes of roughness ➔ a good indicator for mapping the surfaces contributing to runoff

Sensitivity of radar signal to soil roughness

- Radar signal backscattered by a bare soil increases with *Hrms* according to a logarithmic or exponential law to then becomes constant after a certain roughness threshold (depends on the wavelength and the radar's incidence angle).

- Several studies show saturation of the radar signal after *k.Hrms* below roughly 1. This threshold corresponds to *Hrms* values of 4 cm in L-band, 1 cm in C-band, and around 0.5 cm in X-band.

- The dynamic of the radar backscattering coefficient is weaker in the case of weak incidence angles (variation of 7 dB for 20º-25º) than in the case of strong incidence angles (variation of 10 dB for 45º-50º).

- Theoretical and experimental works show a slightly stronger sensitivity of the signal to the roughness of bare soil in HH polarization.

- Only large wavelengths (e.g. L-band) and strong incidence angles (e.g. 45º) allow to map three roughness classes (smooth "sowing," rough "great plowed soil," moderately rough "small plowed soil") [BAG 02].

Soil roughness mapping

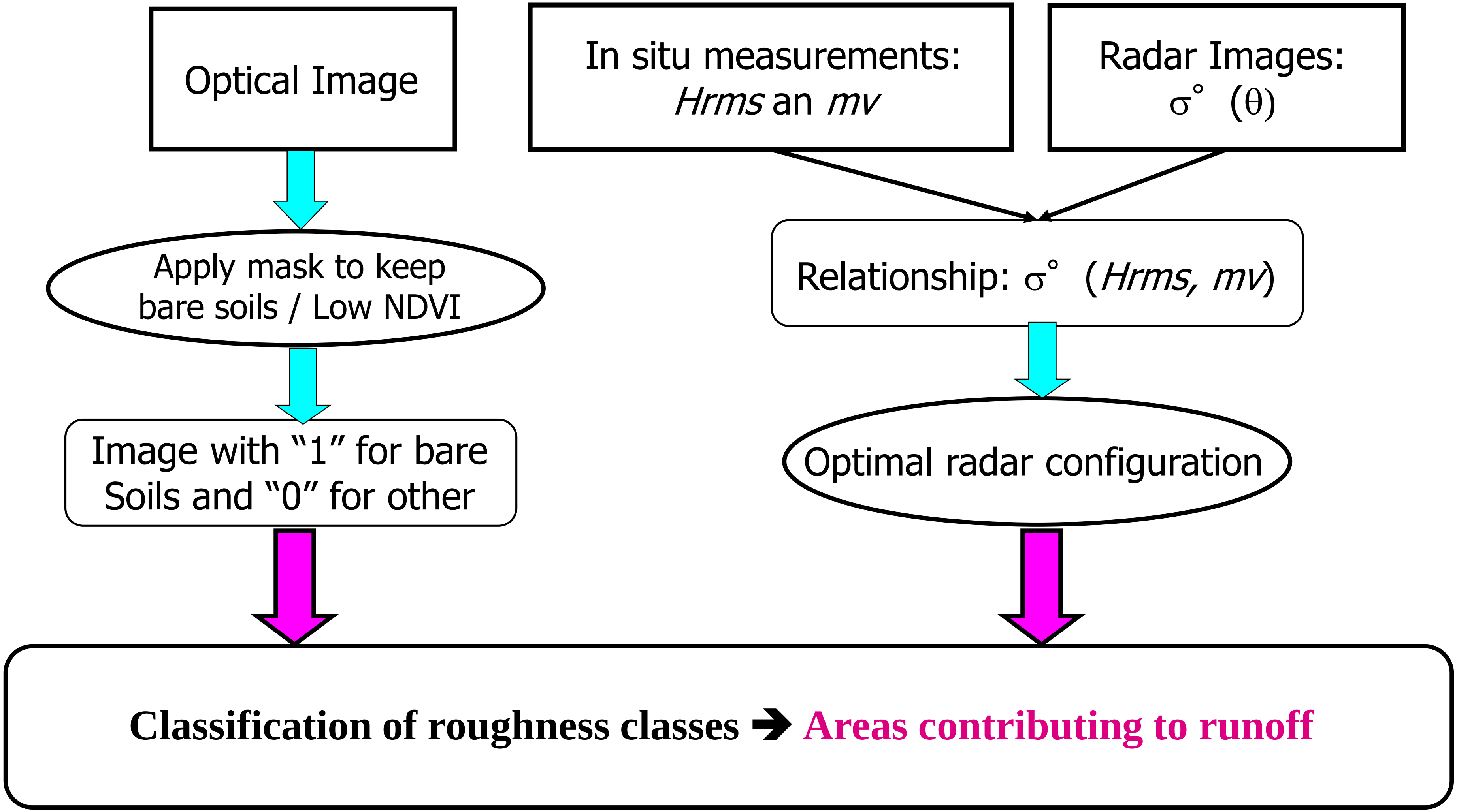

θ: incidence angle
Hrms: roughness
mv: soil moisture

Areas contributing to runoff

Use of radar images for the mapping of surfaces potentially contributing to runoff in an agricultural context:

- Low roughness: High runoff potential
- High roughness: Low runoff potential

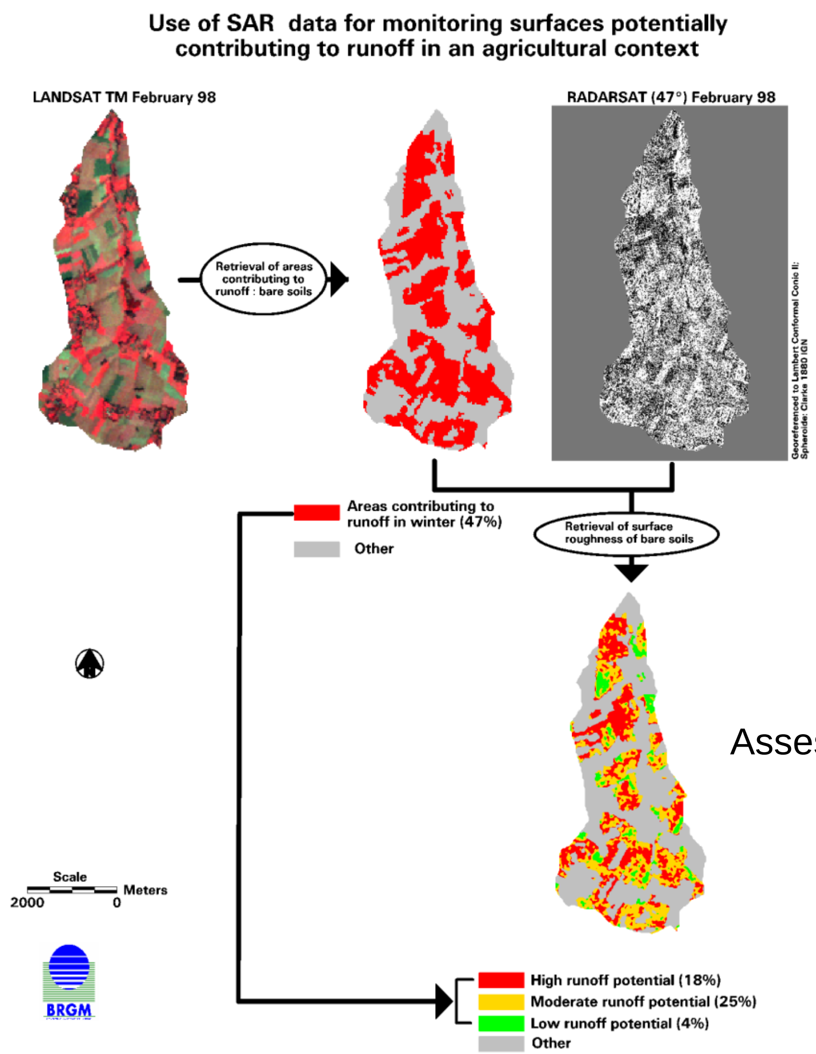

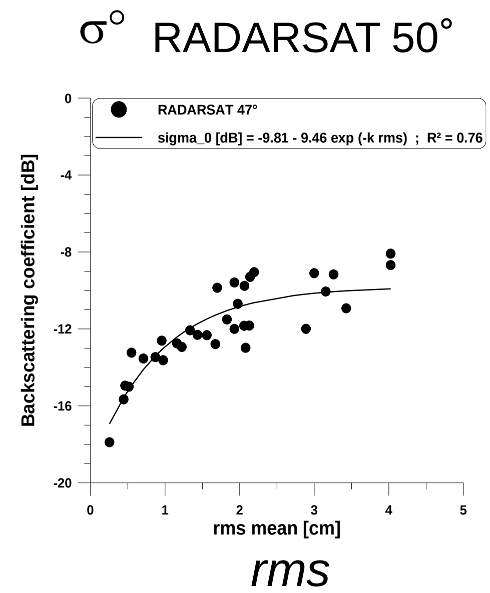

Assess to areas contributing to runoff

3.2.2 Sensitivity of radar signal to soil moisture

Interest of soil moisture

- Spatio-temporal monitoring of soil moisture in agricultural areas is of great importance for various applications: agriculture, hydrology, risks…
- The use of in situ sensors makes it possible to ensure monitoring, but this technique is very expensive and can only be carried out on a very small agricultural sector, hence the importance of spatial remote sensing, which today allows operational and large-scale mapping of soil moisture, with high spatio-temporal resolution.
- Early work to estimate and map surface moisture with radar imagery was done primarily on bare soils.
- In the presence of vegetation, the coupling of radar and optical data is essential to be able to estimate the soil moisture. Indeed, optical data are complementary to radar data, and their interest lies in their potential to estimate the physical parameters of vegetation, for example the Normalized Difference Vegetation Index (NDVI) or the foliar (Leaf Area Index, LAI)

Soil moisture and radar signal

- The radar signal increases with soil moisture

13/02/08

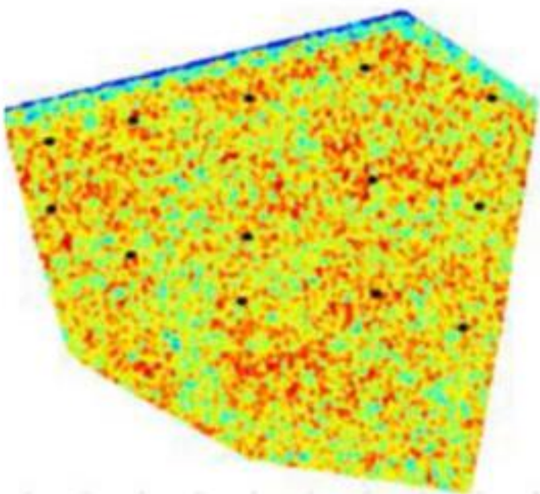

High moisture

13/05/08

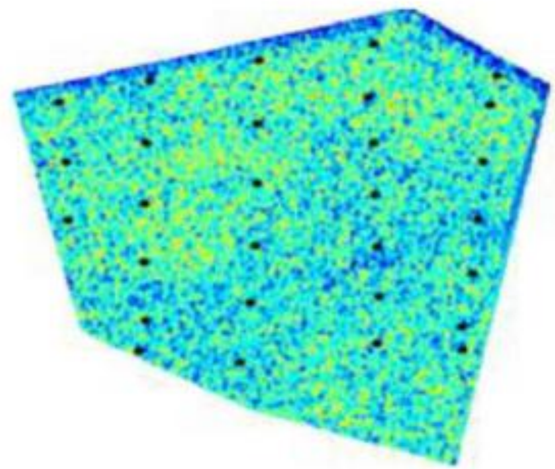

Low moisture

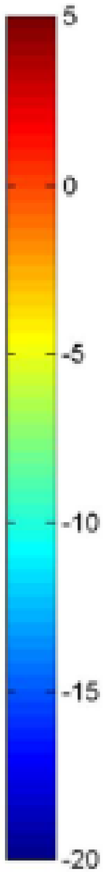

$\sigma°$ in dB

Soil moisture and radar signal

(a) : C-(20°-24°)
(b) : C-(43°-45°)
(c) : X-(25°-28°)
(d) : X-(50°-52°)

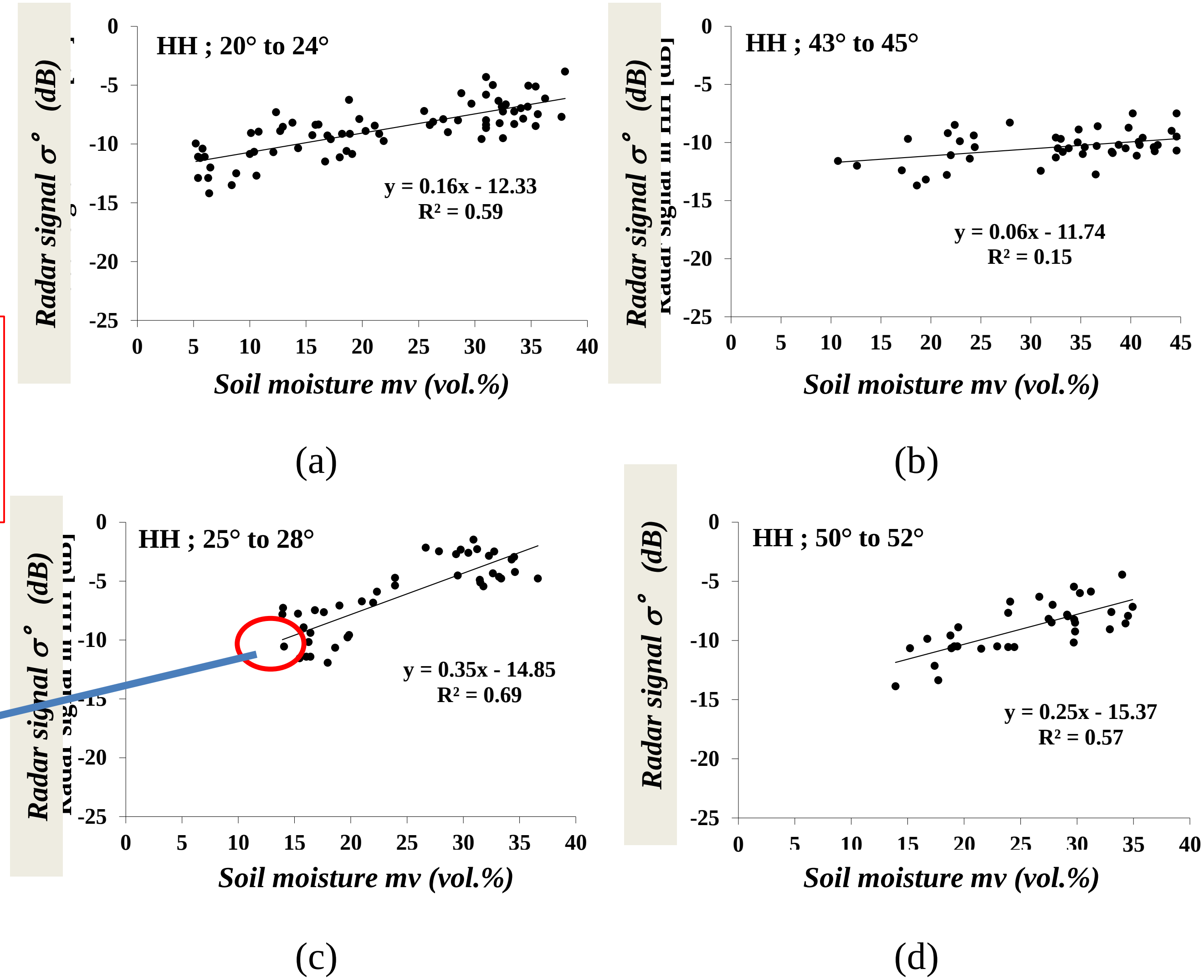

In X-axis: mean of mv measurements
In Y-axis: mean of radar signal over a reference plot

- **Better sensitivity of radar signal to soil moisture at low incidence angle and for low λ (high radar frequencies)**

Soil moisture and radar signal

- Dry surfaces → weak radar signal
- Wet surfaces → strong radar signal
- The signal increases with humidity according to a logarithmic law for humidity not exceeding 35-40 vol.% (this value corresponds to a saturated soil)
- This logarithmic function corresponds to a linear function for humidity between 10 and 35 vol.%
- From moistures of 35-40 vol.% (we begin to have water in a free state because the soil is saturated), the radar signal stops increasing and then begins to decrease with increasing moisture. Thus, the estimation of the surface moisture is no longer possible without ambiguity after this moisture threshold of 35-40 vol.%

Soil moisture and radar signal

- **The sensitivity of radar signal to soil moisture (*S*) decreases when the incidence angle or the radar wavelength increases!**

  - ✓ Optimal radar configuration radar for a better sensitivity of radar signal to moisture ➔ low incidence (15° -35°)

  - ✓ In C-band (Sentinel-1), *S* ~ 0.15 dB/vol.% for θ = 35° . For θ = 20° -25° , *S* ~ 0.2 dB/vol.% ➔ <u>this means that the C-band radar signal increases by about 1 dB if the humidity increases by 5 vol.%</u>

  - ✓ *S* is twice as high in X band (λ=3 cm) than in C band (~0.35 dB/vol.% in X-band versus 0.15 dB/vol.% in C band)

  - ✓ *S* is of the same magnitude in L and C bands

- S is better at low θ or at low λ because the influence of the soil roughness is low

Sensitivity of radar signal to soil moisture

- Optimal configuration for obtaining the best sensitivity of the radar signal to soil moisture (weak influence of the roughness): HH polarization and a weak radar incidence angle: 15º-35º
- Simulations illustrate an approximately logarithmic law between soil moisture and the radar signal.
- This logarithmic function is generally approximated by a linear function for soil moisture between 10 and 35 vol. %.
- After a soil moisture of around 35 vol. %, the radar signal stabilizes, then starts to decrease with the increase of soil moisture, so the estimation of soil moisture cannot be done without ambiguity after this threshold of around 35 vol. %.
- In C-band, sensitivity of radar signal to soil moisture, approximately between 0.15 dB/vol.% and 0.3 dB/vol. %.
- The signal's sensitivity to soil moisture is twice as high in X-band as in C-band (~0.35 dB/vol. % in X-band vs. 0.15 dB/vol. % in C-band).
- Observations in L-band have approximately the same range of sensitivity to soil moisture as in C-band.
- The sensitivity of the signal to soil moisture decreases when the incidence angle increases.

3.2.3 Sensitivity of radar signal to soil salinity

Soil salinity and radar signal

- Salinization is a chemical process that leads to the degradation of arable soil, desertification, and biomass reduction.

- Despite the dominant effect of moisture and roughness on the radar signal, salinity also has a significant effect.

- The influence of salinity is more pronounced on the imaginary part than on the real part of the dielectric constant ε.

- In the imaginary part (ε''), the influence of soil salinity is coupled with moisture. The higher the moisture content, the stronger the effect of salinity on ε''. This is mainly due to the solubility of salts in water leading to an increase in the electrical conductivity of the soil, thus leading to an increase in the imaginary part.

Soil salinity and radar signal

- Few experimental works has been done for the estimation of salinity from radar images.

- Simulations of the radar backscatter coefficient show an increase in the simulated signal with increasing salinity.

- The optimal configurations for salinity estimation from radar data are wet soils, low frequency (e.g. L-band), strong incidence angle and VV polarization (Lasne et al., 2008).

Soil salinity and radar signal

➢Radar backscatter coefficient simulated by the Integral Equation Model (IEM) in L-, C-, and X-bands (40° incidence) as a function of soil water status for two salinity conditions (S=0 and S=100‰):

➔ A potential for salinity estimation only in L-band: The radar signal increases by 2 dB when moving from zero salinity (S=0‰) to saline soil (S=100‰) for moisture > 15 vol.%.

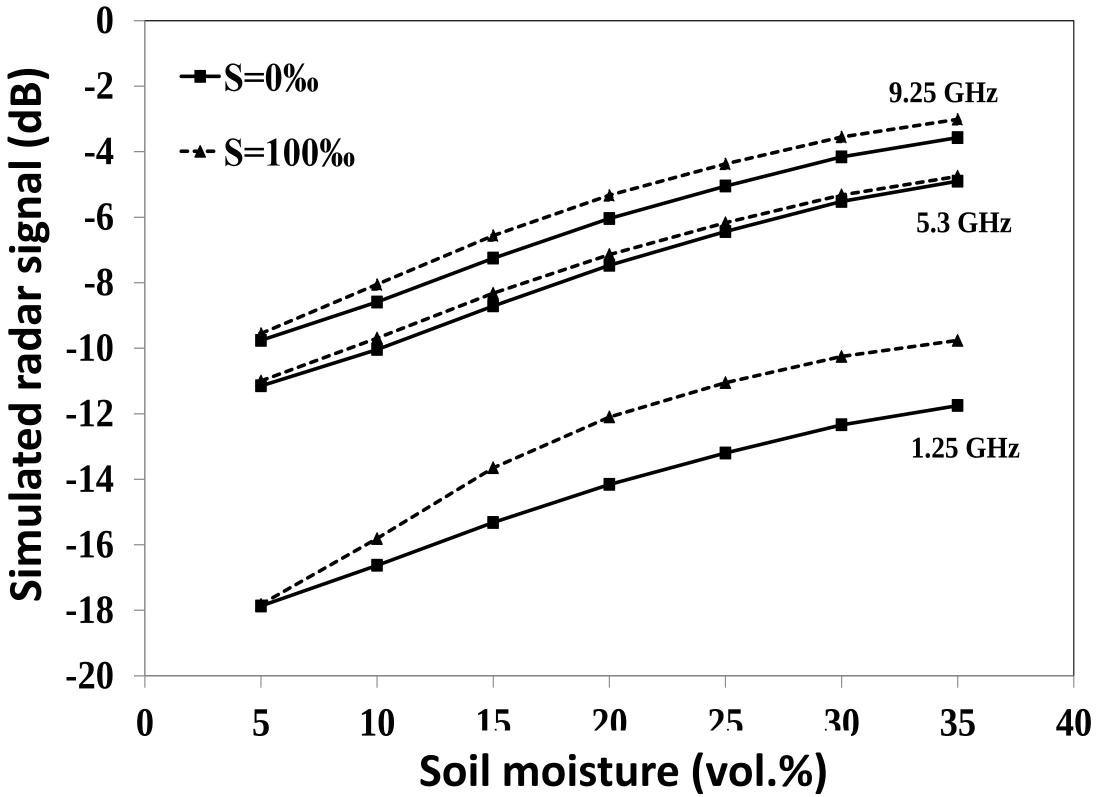

3.2.4 Sensitivity of radar signal to soil freezing

Soil freezing and radar signal

- The results show that the radar backscatter coefficient decreases when the soil temperature falls below 0° C

- A difference of at least 2 dB is observed in C-band between unfrozen and frozen soils (Baghdadi et al., 2018)

- Both VV and VH polarizations provide good detection of frozen soils but that the sensitivity of VH is about 1.5 dB higher

- Discrimination of frozen soils decreases slightly with decreasing soil moisture

➔ The difference between a reference image acquired without frost and an image acquired under frost conditions is a good tool for detecting frozen soils.

Soil freezing and radar signal

➢Analysis of Sentinel-1 radar signal behavior over a wheat field (C, VV and VH):

✓$\sigma°$ VV decreases by 3-4 dB for dates of heavy frost (soil temperature ~ -3.7° C): between Jan. 18 and 26, 2017.

✓A slight decrease of about 1.5 dB was also found in $\sigma°$ VV when the ground was slightly frozen (Feb 11, 2017, ground temperature = -0.6° C).

✓ The difference between $\sigma°$VH of unfrozen soil and $\sigma°$VH of frozen soil is 1 to 2 dB greater than the results obtained with VV polarization.

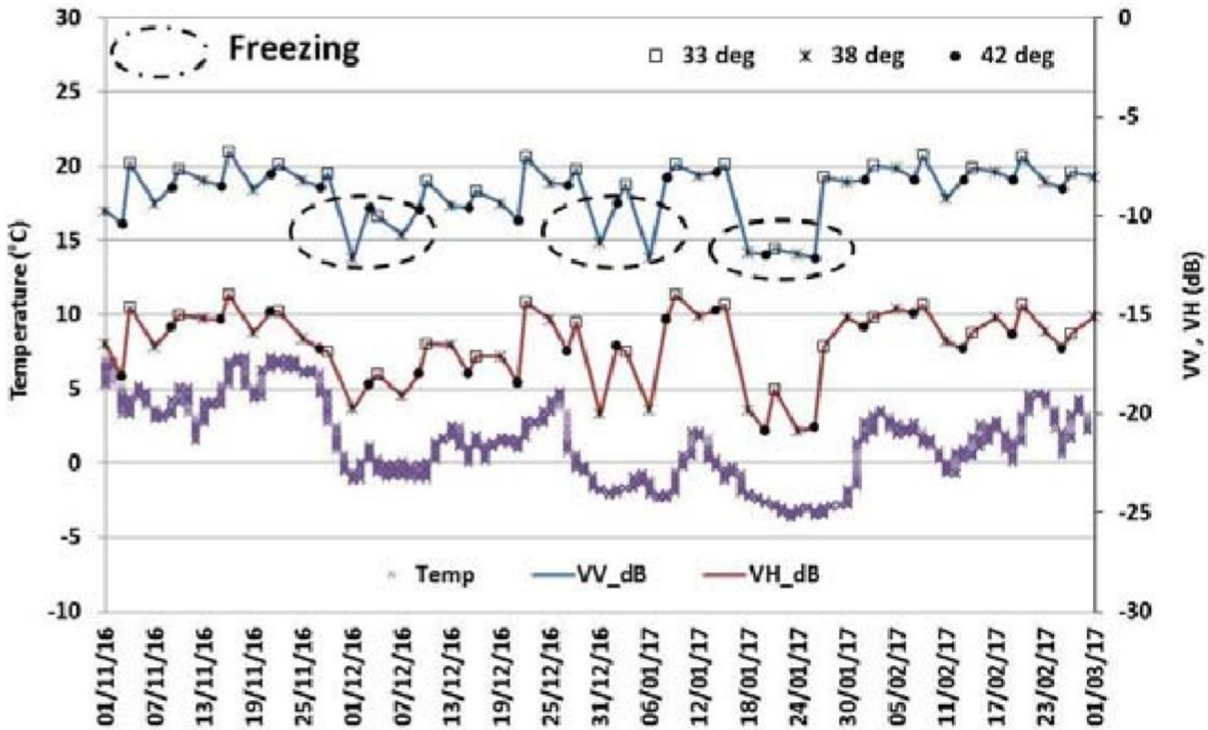

4. Modeling of the radar signal

4.1 Bare soil case

Modeling of radar backscattering on bare soil

- Numerous radar backscattering models have been developed to analyze the radar signal's sensitivity to the soil's physical parameters (roughness and water content in particular) and instrumental parameters (frequency, incidence and polarization).

➔ In order to define the best radar configuration for estimating soil parameters: wavelength choice, pertinence of multi-polarization and polarimetric modes as compared to a mono-polarization mode.

- Different physical analytical models have been developed to simulate radar backscattering of the soil's surface ➔ limited to domains of validity due to the considered physical approximations:
  - the Small Perturbation Model aqdapted to surfaces with a low roughness

$$k.Hrms < 0.3 \qquad\qquad \sqrt{2}Hrms / L < 0.3$$

  - the IEM (*Integral Equation Model*) model developed by Fung et al.

$$kHrms < 3 \qquad\qquad \left((k\,Hrms\cos\theta)^2 / \sqrt{0.46k\,L}\right)\exp\left\{-\sqrt{0.92\,k\,L(1-\sin\theta)}\right\} < 0.25$$

  - …

Modeling of radar backscattering on bare soil

- Semi-empirical models: Dubois, Oh, Baghdadi, …

- In most semi-empirical models, soil roughness, unlike physical models, is parameterized only by the standard deviation of heights (Hrms)

- These models cover much more important ranges of validity than those of physical models and they are better adapted to an operational use for the inversion of radar data.

Description of the Dubois model

$$\sigma^0_{HH} = 10^{-2.75}\left(\frac{\cos^{1.5}\theta}{\sin^5\theta}\right)10^{0.028\,\varepsilon_r \tan\theta}\left(k\,Hrms\sin\theta\right)^{1.4}\lambda^{0.7}$$

$$\sigma^0_{VV} = 10^{-2.35}\left(\frac{\cos^{3}\theta}{\sin^3\theta}\right)10^{0.046\,\varepsilon_r \tan\theta}\left(k\,Hrms\sin\theta\right)^{1.1}\lambda^{0.7}$$

k: radar wave number (*k*), *Hrms* the soil's volumetric water content (*mv*)

Domain of validity is:

$k\,Hrms \leq 2.5$

$mv \leq 35$ % vol.

$\theta \geq 30^{\circ}$

Modeling of radar backscattering on bare soil

Description of the Oh model:

- Oh *et al.* developed a semi-empirical backscattering model with numerous versions between 1992 and 2004.

- $p = \sigma^\circ_{HH} / \sigma^\circ_{VV}$, $q = \sigma^\circ_{HV} / \sigma^\circ_{VV}$ and σ°_{HV} are defined as:

$$p = 1 - \left(\frac{\theta}{90^\circ}\right)^{0.35\, mv^{-0.65}} e^{-0.4 (k\, Hrms)^{1.4}}$$

$$q = 0.095\,(0.13 + \sin 1.5\theta)^{1.4}\left(1 - e^{-1.3 (k\, Hrms)^{0.9}}\right)$$

$$\sigma^0_{HV} = 0.11\, mv^{0.7} \cos^{2.2}\theta \left(1 - e^{-0.32 (k\, Hrms)^{1.8}}\right)$$

k: radar wave number (k), *Hrms* the soil's volumetric water content (mv)

Oh model's domain of validity is:

$0.13 < k\, Hrms \leq 6.98$

$4 < mv$ (% vol.) ≤ 29.1

$10^\circ \leq \theta \leq 70^\circ$

Description of the Baghdadi model

- A new semi-empirical radar backscattering model on bare soil surfaces based on the Dubois model using a wide dataset of backscattering coefficients (in X, C and L bands) extracted from SAR (synthetic aperture radar) images and in situ soil surface parameter measurements (moisture content and surface roughness):

- The radar signal in polarization pq (=HH, VV and HV) is the product of a function that depends on θ, a function that depends on mv and a third function that depends on the roughness (in linear scale) :

$$\sigma^{\circ}_{pq} = f_{pq}(\theta)\; g_{pq}(mv, \theta)\; \Gamma_{pq}(kHrms, \theta)$$

Description of the Baghdadi model

- After optimizing, we have:

$$\sigma^{\circ}_{HH} = 10^{-1.287} (\cos\theta)^{1.227}\ 10^{0.009\, cotan\,(\theta)\, mv}\ (kHrms)^{0.86\, \sin(\theta)}$$

$$\sigma^{\circ}_{VV} = 10^{-1.138} (\cos\theta)^{1.528}\ 10^{0.008\, cotan\,(\theta)\, mv}\ (kHrms)^{0.71\, \sin(\theta)}$$

$$\sigma^{\circ}_{HV} = 10^{-2.325} (\cos\theta)^{-0.01}\ 10^{0.011\, cotan\,(\theta)\, mv}\ (kHrms)^{0.44\, \sin(\theta)}$$

θ: incidence angle, expressed in radians and *mv* is in vol.%.

The new model shows that this condition is satisfied when:

$20^{\circ} < \theta < 45^{\circ}$

kHrms < 6

mv < 35 vol.%

IEM calibrated by Baghdadi: IEM_B

- IEM is the best known physical model

- Numerous studies have assessed the different radar backscattering models. Most of the time, strong differences have been observed between model simulations and real SAR data able to reach several decibels, making the results of radar signal inversion imprecise. This difficulty of accurately modeling the real radar signal is particularly linked to complexity of describing and measuring the soil's roughness parameters (autocorrelation function, correlation length, and standard deviation of heights) precisely.

- Baghdadi et al. [BAG 06, BAG 11a, BAG 11b, BAG 15] proposed a semi-empirical calibration of the IEM backscattering model with the intention of better reproducing the radar backscattering coefficient of bare soils. This calibration replaced the measured correlation length, which is the least precise roughness parameter, with a forcing parameter. The results showed that the calibration parameter depends on *Hrms*, radar incidence angle (θ), and radar frequency.

IEM calibrated by Baghdadi: IEM_B

The calibration parameter *Lopt* obtained with a Gaussian autocorrelation function is described as follows:

$$\text{In X-band: } \begin{cases} Lopt\,(Hrms,\theta,HH) = 18.102\; e^{-1.891\theta}\; Hrms^{0.7644\, e^{0.2005\,\theta}} \\ Lopt\,(Hrms,\theta,VV) = 18.075\; e^{-2.1715\theta}\; Hrms^{1.2594\, e^{-0.8308\,\theta}} \end{cases}$$

$$\text{In C-band: } \begin{cases} Lopt\,(Hrms,\theta,HH) = 0.162 + 3.006\; (\sin 1.23\,\theta)^{-1.494}\; Hrms \\ Lopt\,(Hrms,\theta,HV) = 0.9157 + 1.2289\; (\sin 0.1543\,\theta)^{-0.3139}\; Hrms \\ Lopt\,(Hrms,\theta,VV) = 1.281 + 0.134\; (\sin 0.19\,\theta)^{-1.59}\; Hrms \end{cases}$$

$$\text{In L-band: } \begin{cases} Lopt\,(Hrms,\theta,HH) = 2.6590\; \theta^{-1.4493} + 3.0484\; Hrms\; \theta^{-0.8044} \\ Lopt\,(Hrms,\theta,VV) = 5.8735\; \theta^{-1.0814} + 1.3015\; Hrms\; \theta^{-1.4498} \end{cases}$$

θ is in radians

Lopt and *Hrms* are in centimeters.

Lopt was obtained with a Gaussian autocorrelation function

This calibration has been performed using numerous databases, acquired at numerous study sites, with different radar sensors (ERS, JERS, RADARSAT, ASAR, PALSAR, TerraSAR-X, COSMO-SkyMed, SIR-C/X), with incidence angles from 23º to 57º, and HH, HV, and VV polarizations.

Estimation of soil parameters: bare soil

Using single SAR configuration : 1 date, 1 polarization, 1 incidence angle

➔ Simple empirical relationships: built using reference data collected on study sites. These reference data refer to in-situ measurements of soil moisture and/or roughness, as well as the mean of the backscattering coefficient on each reference plot calculated using acquired radar images.

- linear for the soil moisture $\sigma^0_{dB} = \alpha\, mv + b_1$
- logarithmic (or exponential) for soil roughness $\sigma^0_{dB} = \beta \log(k\, Hrms) + b_2$

➔ Radar backscattering coefficient (in decibels) is defined by a single soil parameter (soil moisture or roughness), while the other soil parameter is assumed to be constant or have little effect on the radar signal (this configuration only allows one soil parameter to be determined at a time).

➔ SAR sensors' parameters chosen to increase the signal's sensitivity to the soil parameter to be estimated (e.g. moisture) and to minimize the effect of the other soil parameters (e.g. roughness).

Estimation of soil parameters: bare soil

Using multi-incidence SAR data: one image with a weak incidence (θ_{weak}~20°) and one image with a strong incidence (θ_{strong}~40°).

$$\begin{cases} \sigma^0(\theta_{weak}) = \alpha_1\, mv + \beta_1 \log(k\,Hrms) + c_1 \\ \sigma^0(\theta_{strong}) = \alpha_2\, mv + \beta_2 \log(k\,Hrms) + c_2 \end{cases}$$

By replacing the term $\log(k\,Hrms)$ in $\sigma^0(\theta_{weak})$ with the one $\sigma^0_{dB}(\theta_{strong})$, the soil moisture can be estimated using the following relation:

$$mv = A\sigma^0(\theta_{weak}) + B\sigma^0(\theta_{strong}) + C$$

Several studies used the relation $\sigma^0(\theta_{weak})/\sigma^0(\theta_{strong})$ when formulating the inversion procedure because of this relation's maximum sensitivity to soil roughness [ZRI 03]:

$$mv = A\sigma^0(\theta_{weak}\ or\ \theta_{strong}) + B\left(\frac{\sigma^0(\theta_{weak})}{\sigma^0(\theta_{strong})}\right)_{dB} + C$$

The roughness parameter *Hrms* can be estimated by using the relation:

$$Hrms = \frac{1}{k}\,10^{D\sigma^0(\theta_{weak}) + E\sigma^0(\theta_{strong}) + F}$$

Estimation of soil parameters: bare soil

<u>Using multi-polarization SAR data: 2 polarizations, same date, same sensor, same acquisition</u>

- Two polarizations does not improve the estimation of soil moisture, for example, in comparison with cases where a single polarization is used. In fact, the improvement is less than 1 vol. % [BAG 06].

<u>Using polarimetric SAR data: HH, HV, VH, VV</u>

- Hajnsek et al. [HAJ 03] have shown that entropy and the alpha angle (derived from the Cloude decomposition) in L-band increase with soil moisture and that anisotropy is independent of the soil moisture. Furthermore, it has been shown that entropy increases with *Hrms*, that the alpha angle is independent of *Hrms*, and that when *k.Hrms* increases to 1, anisotropy decreases in an almost linear way.

- Contrary to the results obtained in L-band, the results obtained in C-band show that the use of polarimetric parameters (entropy, alpha angle, anisotropy …) do not significantly improve the estimation of the soil moisture and roughness in comparison with methods that only use the backscattering coefficients in polarizations HH, HV, or VV [BAG 12b].

Estimation of soil parameters: bare soil

Using multi-date SAR data

- Two polarizations does not improve the estimation of soil moisture, for example, in comparison with cases where a single polarization is used. In fact, the improvement is less than 1 vol. % [BAG 06].

- In order to estimate the soil moisture in semi-arid zones, where it can be assumed that the soil roughness is constant throughout the year, the difference ($\Delta\sigma^{\circ}$) between an image from the wet season and an image from the dry season is used (effects of roughness are eliminated):

$$\Delta\sigma^{\circ}_{dB} = \alpha\,(mv_{wet\ season} - mv_{dry\ season}) = \alpha\,\Delta mv$$

4.2 Case of agricultural soils with vegetation

Estimation of soil parameters: soils with vegetation

- Spatial and temporal monitoring of soil moisture on plots with vegetation cover is a key parameter for different applications, especially for irrigation management.

- Different physical and semi-empirical models have been developed to quantify the contribution of the vegetation in the received radar signal in order to extract the soil contribution and estimate its moisture.

- The most widely used model is the Water Cloud Model (WCM): a very simple but very efficient semi-empirical model developed by Attema and Ulaby (1978).

Water Cloud Model (WCM)

Soil with vegetation

$$\sigma^0_{tot} = \sigma^0_{veg} + T^2\, \sigma^0_{soil}$$

$$\sigma^0_{veg} = A.V_1.\mathrm{Cos}\,\theta\ \ (1 - T^2)$$

$$T^2 = \mathrm{Exp}\,(-2.B.V_2.\sec\theta)$$

$$\sigma^0_{soil} = C(\theta)\,\exp\,(D.M_v)$$

- σ^0_{tot} **:** Total backscattered radar signal (linear unit)
- $\boldsymbol{\sigma^0_{veg}}$ **:** Vegetation contribution (linear unit)
- $\mathbf{T^2}$ **:** Two-way attenuation
- $\boldsymbol{\sigma^0_{soil}}$ **:** Soil contribution (linear unit)
- $\mathbf{V_1 = V_2}$ **:** Vegetation descriptors (BIO (kg/m^2), VWC (kg/m^2), HVE (m), LAI (m^2/m^2), NDVI …)
- **θ :** Radar incidence angle; $\sec(\theta) = 1/\cos(\theta)$
- **A et B:** Parameters depending on the canopy descriptors and radar configurations
- $\mathbf{M_v}$**:** Volumetric soil moisture (Vol.%)
- **C:** dependent on roughness and incidence angle
- **D:** sensibility of radar signal to $\mathbf{M_v}$ in the case of bare soils, dependents on radar configurations

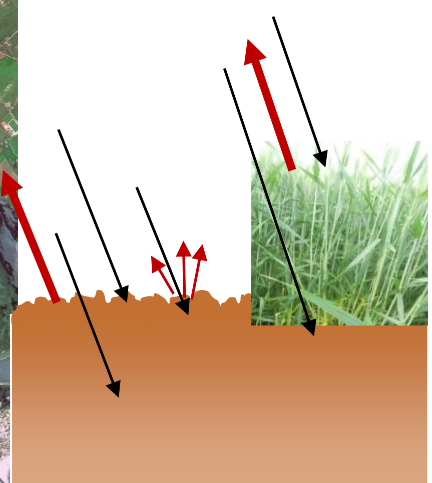

Multiple soil-vegetation diffusions (often neglected)

Water Cloud Model (WCM)

- The soil contribution can be simulated from a physical model (IEM), by a semi-empirical model (Oh, Dubois, Baghdadi), or by using a simplified expression of the soil contribution that takes into account the soil moisture and roughness (in linear scale):

$$\sigma^o_{sol} = C\, e^{D\, mv}$$

- C is a parameter that depends on the soil roughness and the radar configuration.

- D is the sensitivity of the radar signal (linear unit) to bare soil moisture (it depends on the radar configuration).

- This expression assumes that the soil signal is the sum of a contribution related to the soil moisture (in dB), and another related to the roughness (in dB).

Water Cloud Model (WCM)

- Data σ° from SAR images, field measurements of soil parameters (moisture and roughness, or moisture alone if the effect of roughness is neglected), and measurements on vegetation descriptors (in situ or from imagery, optical in particular) are needed to fit the WCM model and estimate the A, B, C, and D parameters.

- Baghdadi et al. (Remote Sensing, 2017) calibrated WCM using C-band radar data at two study sites, one in France and one in Tunisia (winter wheat, grassland, and fallow). The soil contribution was modeled using IEM modified by Baghdadi et al. (using Lopt instead of L):

			$V_1 = V_2 = \text{NDVI}$			
Polarization	A_{pq}	B_{pq}	R^2_{pq}	$RMSE_{pq}$ (dB)	$Bias_{pq}$ (dB)	N
pq = VV	0.0950	0.5513	0.55	1.55	0.18	160
pq = VH	0.0413	1.1662	0.63	1.30	−0.17	68

Results : Modeling results

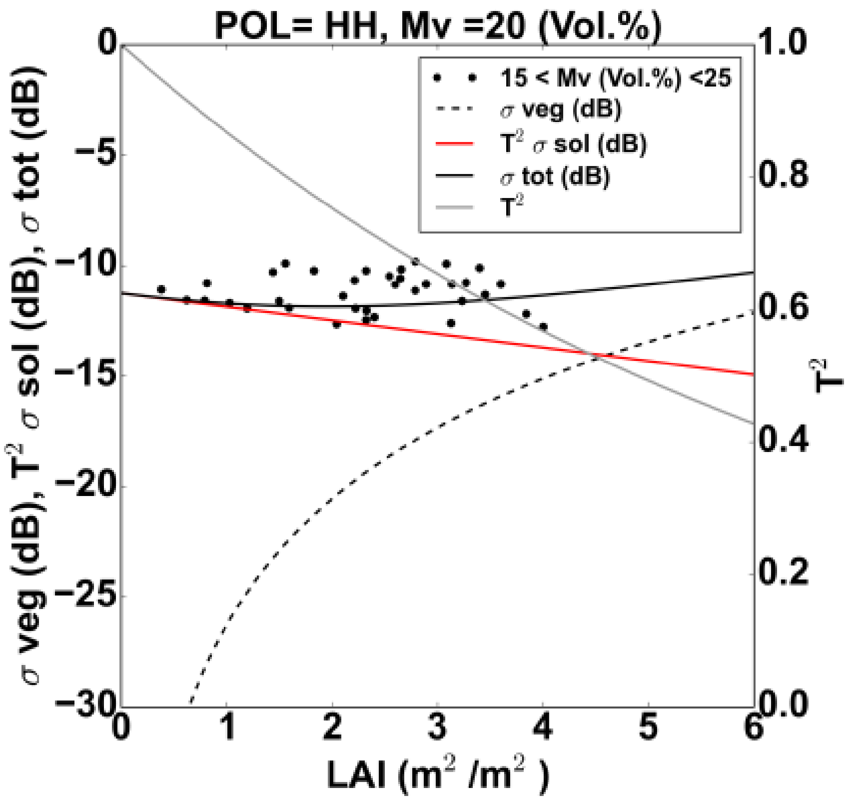

Behaviour of WCM components ($\sigma^\circ_{veg,}$ $T^2\sigma^\circ_{sol}$, and σ°_{tot}) in HH according to LAI.

Black points represent SAR data (σ°_{tot}: validation dataset) associated to M_v measurements situated at ±5 vol. % of the M_v used in the modelling.

Results : Modeling results

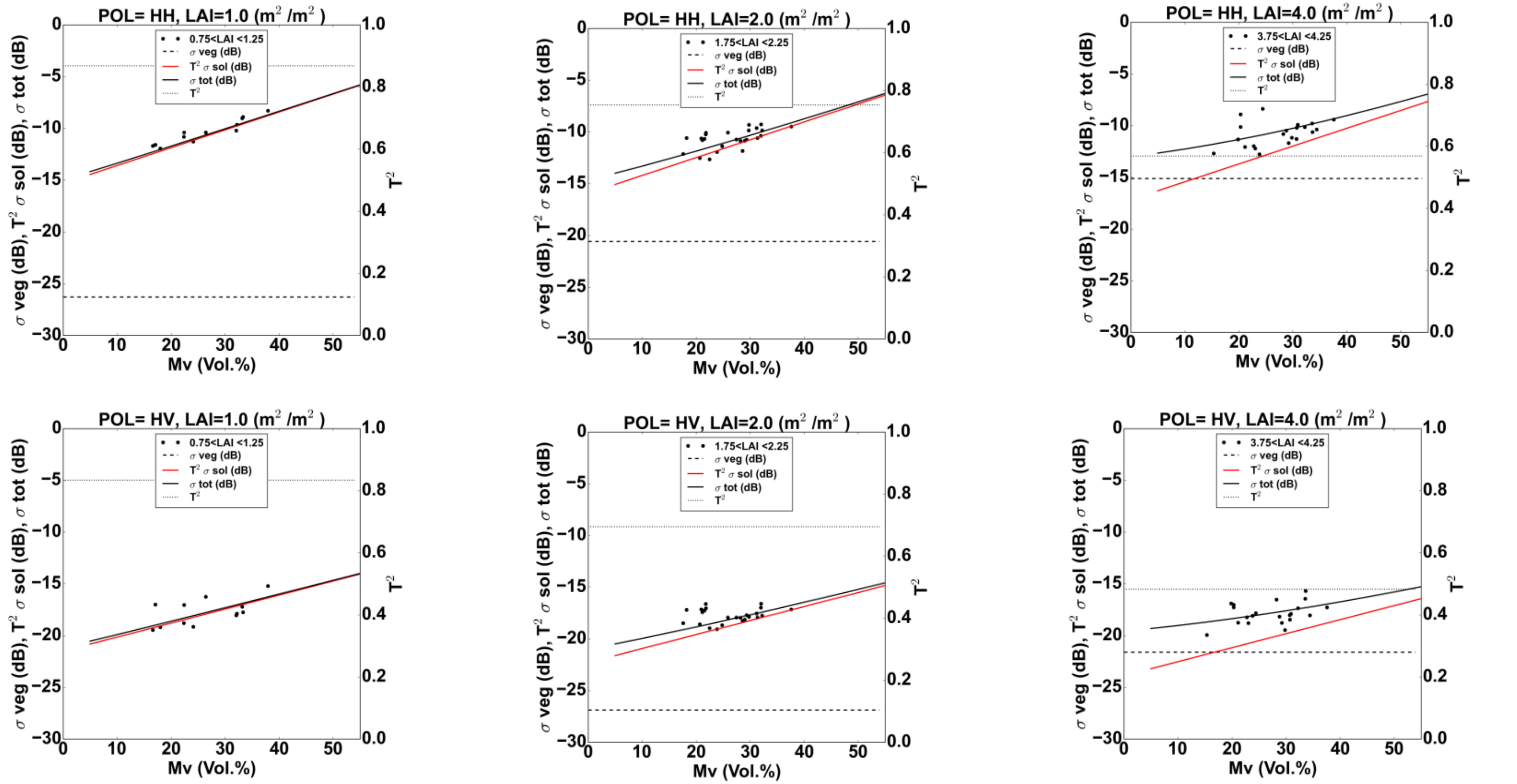

Behaviour of WCM components ($\sigma°_{veg}$, $T^2\sigma°_{sol}$, and $\sigma°_{tot}$) in HH according to M_v.

Black points represent SAR data ($\sigma°_{tot}$: validation dataset) associated to LAI measurements situated at ± 0.25 m^2/m^2 of the LAI used in the modelling.

5. Estimation of soil moisture

Introduction

- Soil moisture mapping in agricultural areas at plot scale is very usefull for many applications such as hydrology, agriculture and risk assessment.

- Currently, several satellite missions provide surface soil moisture estimations at different spatial resolutions (low to medium spatial resolutions):

  - ✓ SMAP: 36 km x 36 km, 9 km x 9 km, 1 km x 1 km
  - ✓ ASCAT: 25 km x 25 km, 12.5 km x 12.5 km, 1 km x 1 km
  - ✓ SMOS: 25 km x 25 km
  - ✓ New: Copernicus Land distributes the first soil moisture estimations over the European continent at 1-km using S1 data: algorithm based on the University of Technology Wien Change Detection Model

Introduction

➢ Sentinel-1 SAR satellites provide C-band SAR data :

- ✓ in free open access mode
- ✓ At high spatial resolution (10 m x 10 m) and high revisit time (6 days)

➔ **encourage the development of an operational algorithm for soil moisture mapping at high spatial resolution**

➢ An operational approach for mapping soil moisture at high spatial resolution (plot scale) in agricultural areas was developed by coupling S1 and S2 images:

- ✓ based on the inversion of the Water Cloud Model (WCM) combined with the modified IEM, and using the neural networks technique
- ✓ **S^2MP: Sentinel-1/Sentinel-2 derived soil Moisture at Plot scale**

Estimation of soil moisture

Simple model with one band (= one information from SAR sensors):

- The simplest empirical model (1 band = one incidence and one polarization):

$$\sigma^0_{dB} = \alpha\, mv + b_1$$

- This expression is built on a given site independently of the roughness for one polarization and a range of incidence angles

- Once this expression constructed from a database (some control plots), the moisture can be estimated everywhere on the same radar image with:

$$mv^{est} = [\sigma^{\circ}\ \ (\mathrm{dB}) - b_1] / \alpha$$

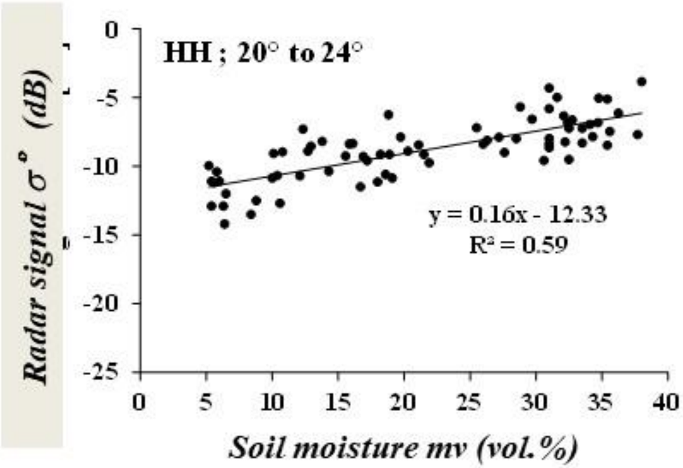

Estimation of soil moisture

- Two bands = 2 wavelengths, 2 angles of incidence or 2 polarizations
- One sensor = 1 wavelength
- One sensor, for a given plot, at a given date = 1 angle of incidence
- One sensor = 1, 2 or 4 polarizations

Estimation of soil moisture

Simple model with two bands:

- Example of radar images acquired at two angles of incidence: a weak angle~20° and a strong angle~40° :

$$\begin{cases} \sigma^0(\theta_{weak}) = \alpha_1\, mv + \beta_1 \log(k\,Hrms) + c_1 \\ \sigma^0(\theta_{strong}) = \alpha_2\, mv + \beta_2 \log(k\,Hrms) + c_2 \end{cases}$$

- In this case, the radar signal is written as the sum of a function that describes the dependence of the signal on moisture and a function that describes the dependence of the signal on roughness (in dB).

- The moisture combining the two images can be written as follows:

$$mv = A\sigma^0(\theta_{weak}) + B\sigma^0(\theta_{strong}) + C$$

- From a database collected [$\sigma^0(\theta_{weak})$, $\sigma^0(\theta_{strong})$, mv]i=1…n on several control plots (n), the parameters A, B and C are estimated and the above equation can be applied to all the agricultural plots of the study site for the estimation of moisture.

Accuracy of mv^{est} from empirical relations

- Case 1: Estimation of mv with a simple linear relationship between $\sigma°$ at one band and mv: relationship valid only for the study site, at a given date, for a given incidence/polarization ➔ unreliable estimate because the effect of roughness is not taken into account (accuracy at best 6 vol.%).

- Case 2: Estimation of mv with a linear relation between $\sigma°$ at 2 incidences and mv: Unlikely to have 2 images acquired at two incidences with stable humidity conditions ➔ If feasible, very good estimate of mv because the effect of roughness is taken into account (accuracy 2 times better than case 1, RMSE on mv ~ 3 vol.%).

- Case 3: Estimation of mv with a linear relationship between $\sigma°$ at 2 polarizations and mv: Quite possible but the $\sigma°$ at the different polarizations are strongly correlated ➔ configuration not very relevant because the accuracy is better only by about 1 vol.% compared to case 1.

Estimation of soil moisture: Neural network

- Our aim was to develop an operational approach for mapping soil moisture at high spatial resolution (up to the plot scale) in agriculture areas by coupling S1 and S2 images.

- The proposed approach is based on the inversion of the Water Cloud Model (WCM) using the neural network (NN) technique.

- The use of the new S1 and S2 data for operational soil moisture mapping in agricultural areas with high revisit time and <u>at the plot scale </u>is an innovative use of spatial imageries

Estimation of soil moisture: Neural network

- Free access to Sentinel data (radar: Sentinel-1 and optical: Sentinel-2) encourages the development of an operational soil moisture mapping algorithm

- The high spatial resolution of Sentinel data (10 m x 10 m) makes it possible to map at the plot level

- Moreover, the high revisit time of S1 (about 15 images per month) makes the moisture product very interesting for many applications: irrigation for example

- An algorithm called S^2MP (Sentinel-1/Sentinel-2 derived soil Moisture at Plot scale) has been developed at UMR TETIS. It reverses WCM combined with IEM modified by Baghdadi (integration Lopt instead of L) and uses neural networks. It has been calibrated on field crop plots (wheat, barley, rape ...) but also on grasslands.

- The code can be downloaded at the reference: **El Hajj M., Baghdadi N., Zribi M., 2018. Estimation de l'humidité du sol par couplage d'images radar et optique. Chapitre book: Baghdadi N., Mallet C., et Zribi M. (eds), QGIS et applications en agriculture et forêt, vol. 2, p. 15-58, 2018, ISTE Editions, 374 pp.**

S^2MP: Description

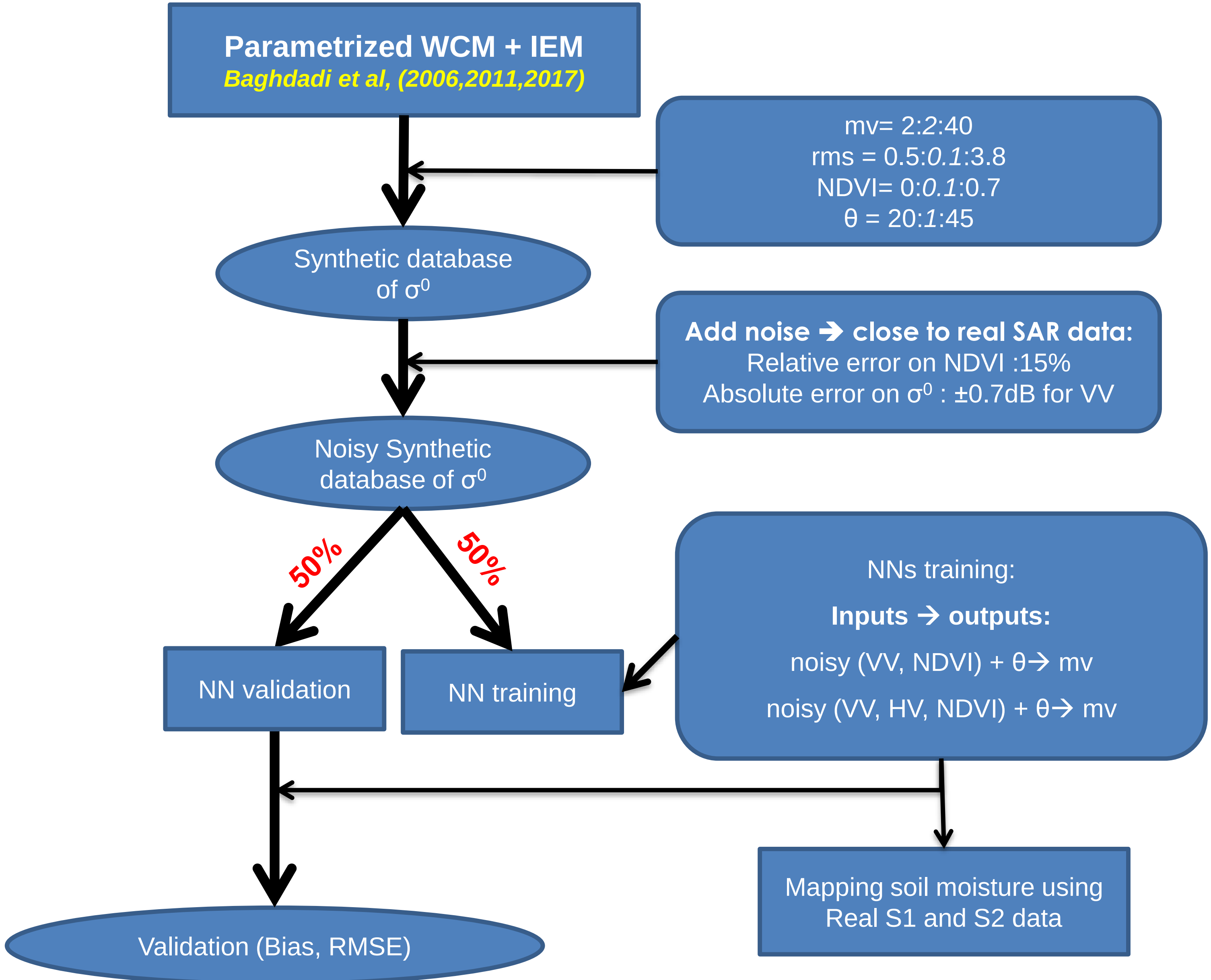

S²MP: accuracy with synthetic Data

NN1 : VV + NDVI+ θ➔ Mv

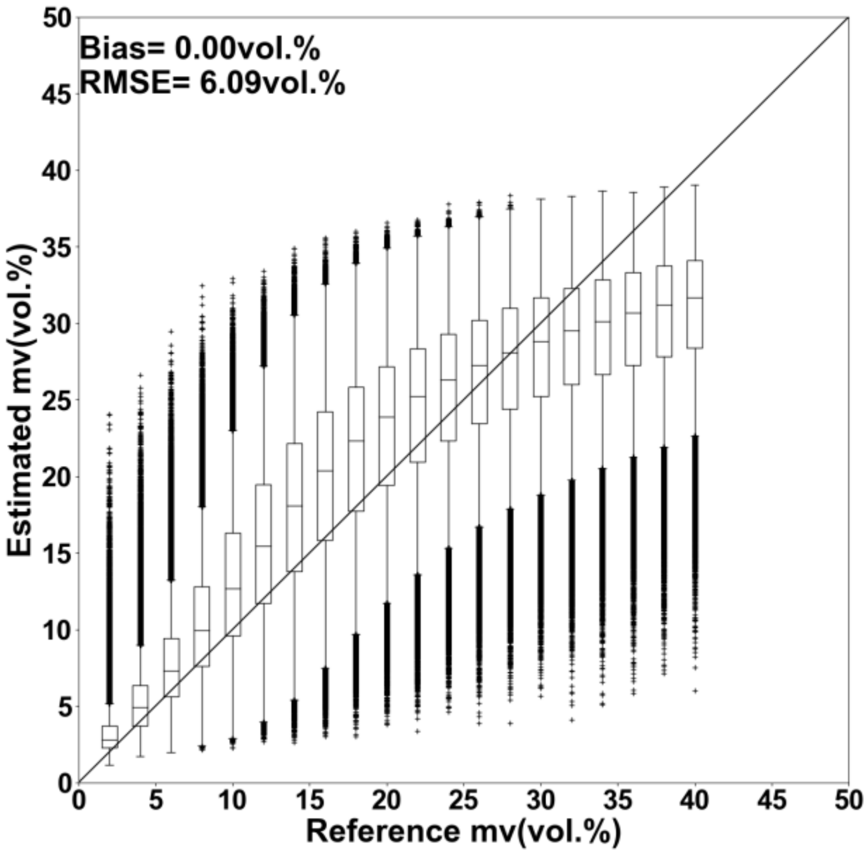

- ✓ mv < 25 vol % : bias = 2.7 vol % & RMSE = 5.5 vol %
- ✓ mv > 25 vol % : bias = −4.1 vol % & RMSE = 6.9 vol%

S²MP: accuracy with synthetic Data

NN1 : VV + NDVI+ θ➔ Mv

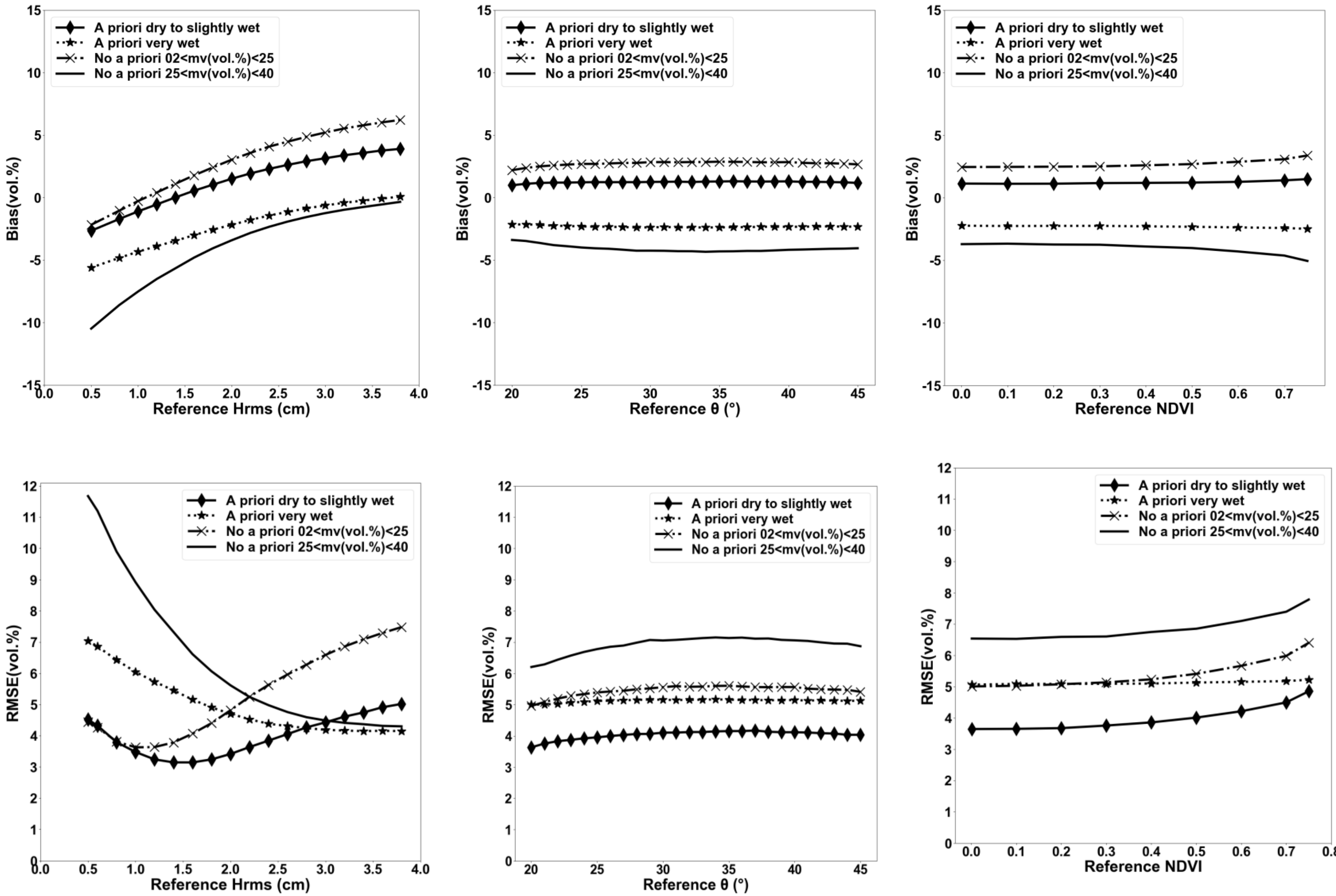

S²MP: accuracy with real Data

NN 1 : VV + NDVI+ θ➔ Mv

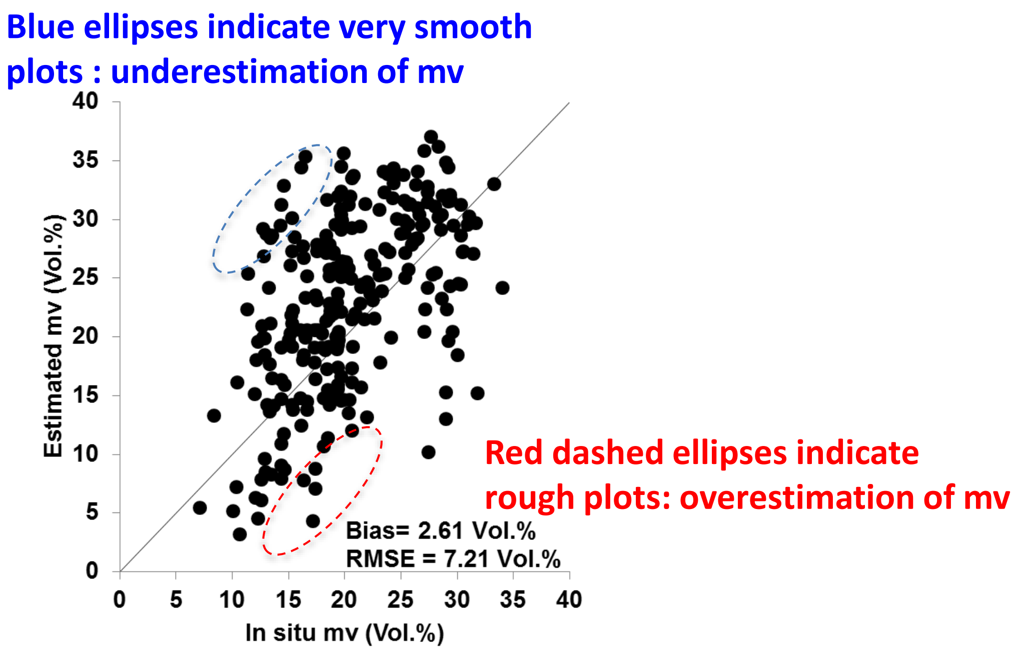

- ✓ Inversion was performed using real SAR data and NDVI derived from optical images
- ✓ Degradation when NDVI is high (mature crops)
- ✓ For some crops, moisture estimation on agricultural plots is no longer possible when vegetation is well developed (NDVI <0.7)

S²MP: soil moisture maps

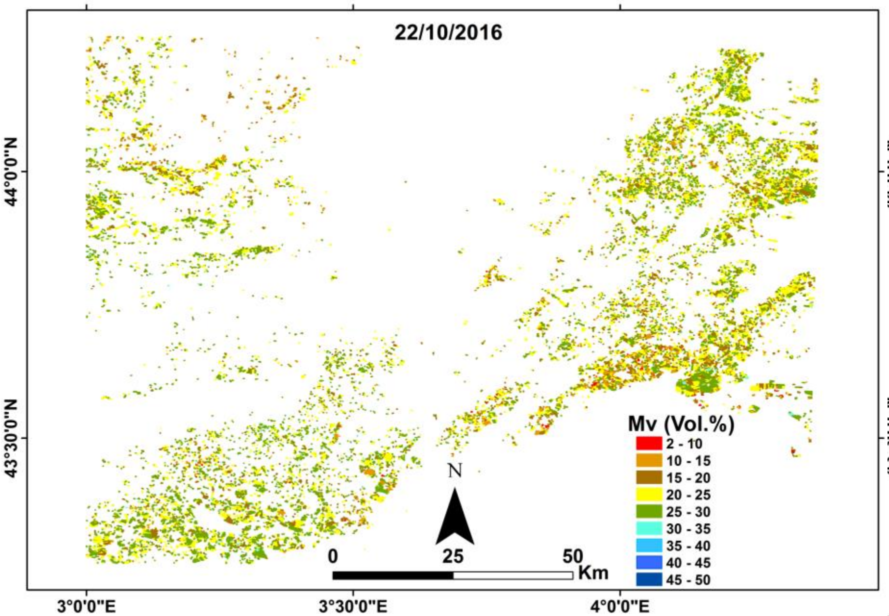

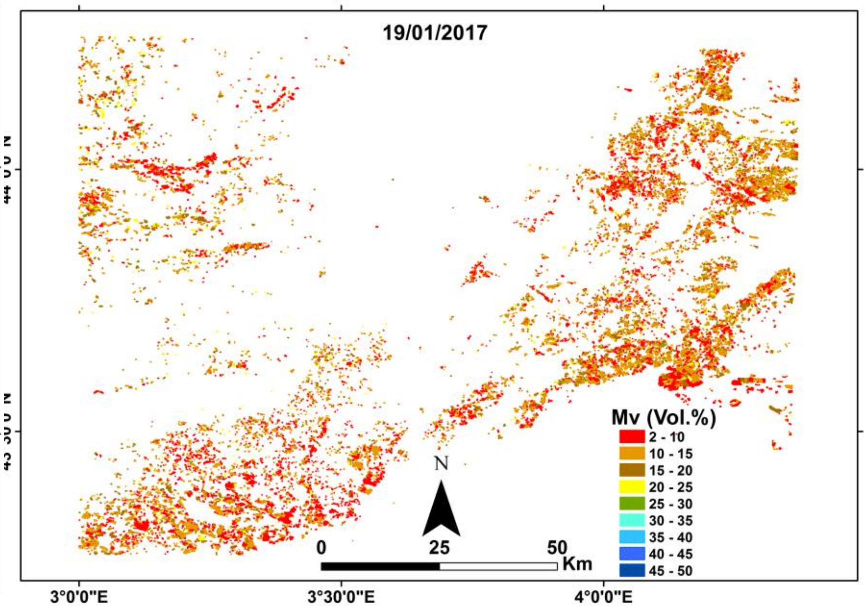

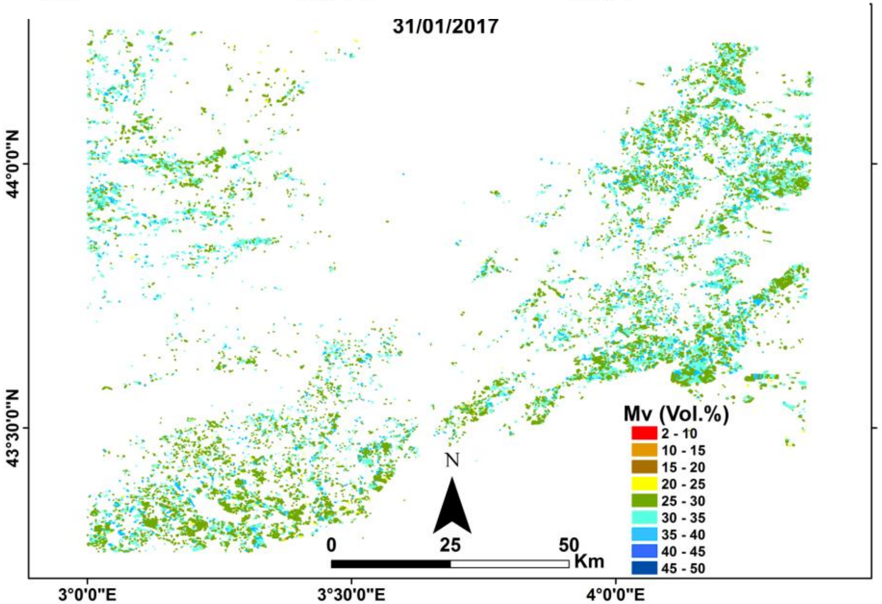

S²MP: soil moisture maps

- Soil moisture maps over many sites in France and in the World (2016-2018, Time : 6 days, plot scale): http://www.theialand.fr/en/thematic-products

- Good coherence observed between the temporal evolution of the soil moisture and the precipitation records

- S1-SM values increases following rainfall event and decreases after a period without rainfall due to evaporation

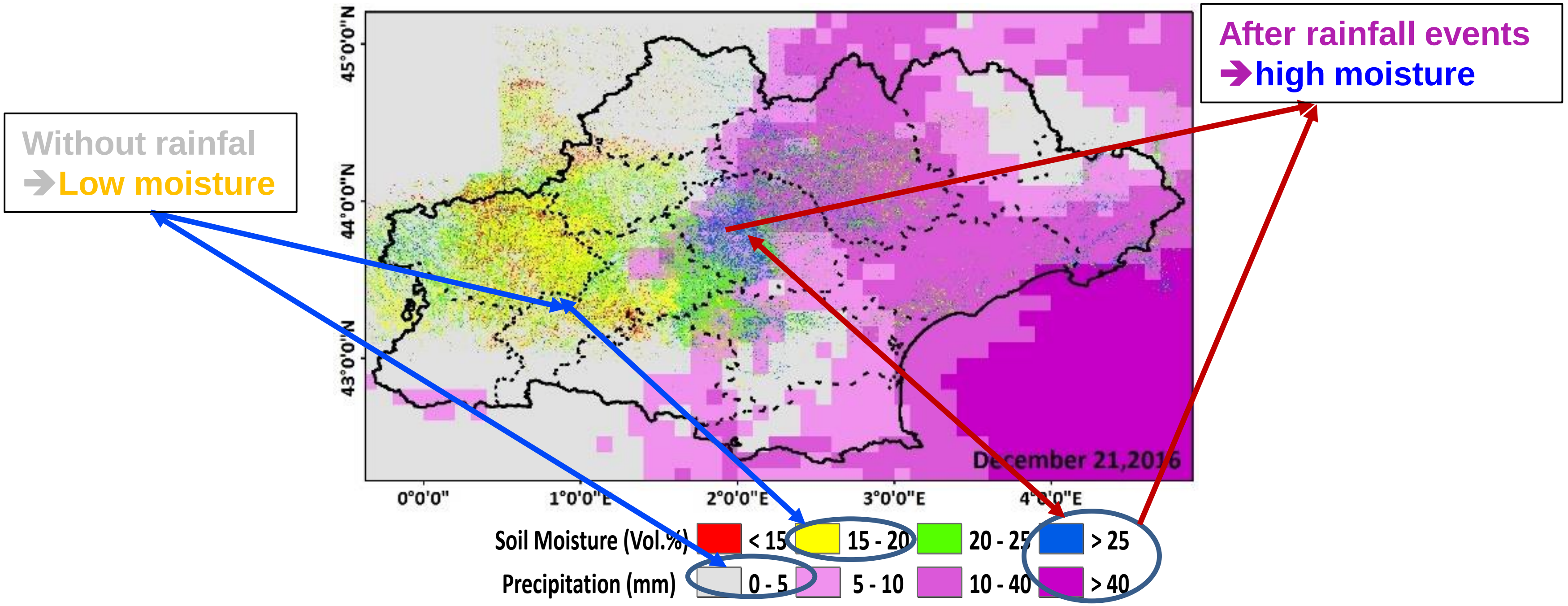

Bazzi et al., RS, 2018

Soil moisture maps on the Theia website

French Land Data Center Theia : https://www.theia-land.fr/en/product/soil-moisture-with-very-high-spatial-resolution/

theia-land.fr/en/product/soil-moisture-with-very-high-spatial-resolution/

Theia

THEIA PRODUCTS EXPERTISE

SOIL MOISTURE AT VERY HIGH SPATIAL RESOLUTION

TABLE OF CONTENT

Data access

Download VHSR Soil Moisture Data on catalogue.theia-land.fr

Download VHSR Soil Moisture Data on Thisme

Read-Me Soil Moisture (Dec. 19) Download

A Python Script to download entire collections

Références bibliographiques

- Attema E.W.P., Ulaby F.T., «Vegetation modelled as a water cloud», Radio Science, 13(2), p. 357–364, 1978.
- Aubert M., Baghdadi N., Zribi M., Douaoui A., Loumagne C., Baup F., El Hajj M., Garrigues S., «Analysis of TerraSAR-X data sensitivity to bare soil moisture, roughness, composition and soil crust», *Remote Sensing of Environment*, 115, p. 1801-1810, 2011.
- Baghdadi N., King C., Bourguignon A., Rmond A., «Potential of ERS and RADARSAT data for surface roughness monitoring over bare agricultural fields : application to catchments in Northern France », *International Journal of Remote Sensing,* 23(17), p. *3427-3442*, 2002.
- Baghdadi N., Holah N., Zribi M., «Calibration of the Integral Equation Model for SAR data in C-band and HH and VV polarizations», *International Journal of Remote Sensing,* 27(4), p. 805-816, 2006.
- Baghdadi N., Cerdan O., Zribi M., Auzet V., Darboux F., El Hajj M., Bou Keir R., «Operational performance of current synthetic aperture radar sensors in mapping soil surface characteristics: application to hydrological and erosion modelling», *Hydrological Processes,* 22(1), p. 9-20, 2008.
- Baghdadi **N.**, Abou Chaaya J., Zribi M., «Semi-empirical calibration of the Integral equation Model for SAR data in C-band and cross polarization using radar images and field measurements», *IEEE Geoscience and Remote Sensing Letters,* 8(1), p.14-18, 2011.
- Baghdadi **N.**, Saba E., Aubert M., Zribi M., Baup F., « Comparison between backscattered TerraSAR signals and simulations from the radar backscattering models IEM, Oh, and Dubois », *IEEE Geoscience and Remote Sensing Letters,* 8(6), p.1160-1164, 2011.

- Baghdadi **N.**, Saba E., Aubert M., Zribi M., Baup F., « Comparison between backscattered TerraSAR signals and simulations from the radar backscattering models IEM, Oh, and Dubois », *IEEE Geoscience and Remote Sensing Letters,* 8(6), p.1160-1164, 2011.
- Baghdadi N., Camus P., Beaugendre N., Malam Issa O., Zribi M., Desprats J.F., Rajot J.L., Abdallah C., Sannier C., «Estimating surface soil moisture from TerraSAR-X data over two small catchments in the sahelian part of western Niger», *Remote Sensing*, 3, p. 1266-1283, doi:10.3390/rs3061266, 2011.
- Baghdadi N., Aubert M., Zribi M., «Use of TerraSAR-X data to retrieve soil moisture over bare soil agricultural fields», *IEEE Geoscience and Remote Sensing Letters*, 9(3), p. 512-516, 2012.
- Baghdadi N., Cresson R., Pottier E., Aubert M., Zribi M., Jacome A., Benabdallah S., «A potential use for the C-band polarimetric SAR parameters to characterise the soil surface over bare agriculture fields», *IEEE Transactions on Geoscience and Remote Sensing,* 50(10), p. 3844-3858., 2012.
- Baghdadi N., Dubois-Fernandez P., Dupuis X., and Zribi M., «Sensitivity of multi-frequency (X, C, L, P and UHF-band) polarimetric SAR data to soil moisture and surface roughness over bare agricultural soils», *IEEE Geoscience and Remote Sensing Letters,* 10(4), p. 731-735, 2013.
- Baghdadi N., Zribi M., Paloscia S., Verhoest N., Lievens H., Baup F., Mattia F., « Semi-empirical calibration of the Integral Equation Model for co-polarized L-band backscattering », *Remote Sensing*, 7, p. 13626-13640, doi: 10.3390/rs71013626, 2015.

- Baghdadi N., El Hajj M., Zribi M., Fayad I., «Coupling SAR C-band and optical data for soil moisture and leaf area index retrieval over irrigated grasslands», *IEEE JSTARS, vol. 9, no. 3, pp. 1229-1243. doi:* 10.1109/JSTARS.2015.2464698, 2015.
- Baghdadi N., Choker M., Zribi M., El Hajj M., Paloscia S., Verhoest N., Lievens H., Baup F., Mattia F., 2016. A new empirical model for radar scattering from bare soil surfaces. *Remote Sensing, vol. 8, Issue 11, pp. 1-14,* doi: 10.3390/rs8110920.
- Baghdadi N., El Hajj M., Zribi M., Bousbih S., 2017. Calibration of the Water Cloud Model at C-band for winter crop fields and grasslands, Remote Sensing, 9, 969; doi:10.3390/rs9090969.
- Baghdadi N., El Hajj M., Choker M., Zribi M., Bazzi H., Vaudour E., Gilliot J.M., Dav M. Ebengo, 2018. Potential of Sentinel-1 images for estimating the soil roughness over bare agricultural soils. Water, 10, 131, pp. 1-14, doi: 10.3390/w10020131.
- Baghdadi N., Bazzi H., El Hajj M., Zribi M., 2018. Detection of frozen soil using Sentinel-1 SAR data. Remote Sensing, 10, 1182, pp. 1-15, doi:10.3390/rs10081182
- Bazzi H., Baghdadi N., El Hajj M., Zribi M., Belhouchette H., 2019. A Comparison of Two Soil Moisture Products S2MP and Copernicus-SSM over Southern France. Journal of Selected Topics in Applied Earth Observations and Remote Sensing, 10 pages
- Bazzi H., Baghdadi N., El Hajj M., Zribi M., 2019. Potential of Sentinel-1 Surface Soil Moisture Product for Detecting Heavy Rainfall in the South of France, Sensors, 2019, 19, 802; doi:10.3390/s19040802

- Bazzi H., Baghdadi N., Ienco D., El Hajj M., Zribi M., Belhouchette H., Escorihuela M.J., Demarez V., 2019. Mapping Irrigated Areas Using Sentinel-1 Time Series in Catalonia, Spain. *Remote Sensing, Remote Sens. 2019, 11, 1836; doi:10.3390/rs11151836.*
- Bousbih S., Zribi M., Lili-Chabaane Z., Baghdadi N., El Hajj M., Gao Q., Mougenot B., 2017. Potential of Sentinel-1 radar data for the assessment of soil and cereal cover parameters, *Sensors*, 17, 2617; doi: 10.3390/s17112617.
- Bousbih S., Zribi M., El Hajj M., Baghdadi N., Lili-Chabaane Z., Gao Q., Fanise P., 2018. Soil Moisture and Irrigation Mapping in A Semi-Arid Region, Based on the Synergetic Use of Sentinel-1 and Sentinel-2 Data, Remote Sensing, 2018, 10(12), 1953
- Bousbih S., Zribi M., Mougenot B., Pelletier C., Lili-Chabaane Z., Baghdadi N., Ben Aissa N., Gorrab A., 2019. Soil texture estimation using radar and optical data from Sentinel-1 and Sentinel-2. Remote Sensing, 2019, 11, 1520
- Choker M., Baghdadi N., Zribi M., El Hajj M., Paloscia S., Verhoest N., Lievens H., Mattia F., 2017. Evaluation of the Oh, Dubois and IEM models using large dataset of SAR signal and experimental soil measurements. *Water*, 9(38), pp. 1-27.
- Dubois P.C., Van Zyl J., Engman T., «Measuring soil moisture with imaging radars», *IEEE Transactions on Geoscience and Remote Sensing*, 33, p. 915-926, 1995.
- El Hajj M., Baghdadi N., Zribi M., Belaud G., Cheviron B., Courault D., Charron F., 2016, «Soil moisture retrieval over irrigated grassland using X-band SAR data», *Remote Sensing of Environment*, *vol. 176, pp. 202-218*

- El Hajj M., Baghdadi N., Cheviron B., Belaud G., Zribi M., 2016. Integration of remote sensing derived parameters in crop models: application to the PILOTE model for hay production. *Agricultural Water Management*, vol. 176, pp. 67-79
- El Hajj M., Baghdadi N., Cheviron B., Zribi M., Angelliaume S., 2016. Analysis of Sentinel-1 radiometric stability and quality for land surface applications. *Remote Sensing*, 8(5), 406, doi:10.3390/rs8050406
- El Hajj M., Baghdadi N., Zribi M., Bazzi H., Synergic use of Sentinel-1 and Sentinel-2 images for operational soil moisture mapping at high spatial resolution over agricultural areas, *Remote Sensing*, 2017, 9, 1292; doi:10.3390/rs9121292
- El Hajj M., Baghdadi N., Zribi M., Rodríguez-Fernández N., Wigneron J.P., Al-Yaari A., Al Bitar A., Albergel C., Calvet J.C., 2018. Evaluation of SMOS, SMAP, ASCAT and Sentinel-1 soil moisture products at sites in Southwestern France, *Remote Sensing*, 10, 569, pp. 1-17, doi:10.3390/rs10040569.
- El Hajj M., Baghdadi N., Zribi M., 2019. Comparative analysis of the accuracy of surface soil moisture estimation from the C- and L-bands. *International Journal of Applied Earth Observations and Geoinformation*, 82(2019), 101888

- El Hajj M., Baghdadi N., Bazzi H., Zribi M., 2019. Penetration analysis of SAR signals in the C and L bands for wheat, maize, and grasslands. Remote Sensing, 2019, 11, 31; doi:10.3390/rs11010031
- Fung A.K., Li Z. Chen K.S., «Backscattering from a randomly rough dielectric surface», *IEEE Transactions on Geoscience and Remote Sensing*, 30, p. 356-369, 1992.
- Gao Q., Zribi M., Escorihuela M.J., Baghdadi N., Synergetic use of Sentinel-1 and Sentinel-2 for soil moisture mapping at 100 m resolution, Sensors 2017, 17, 1966; doi:10.3390/s17091966.
- Gao Q., Zribi M., Escorihuela M.J., Baghdadi N., Segui P.Q., Irrigation mapping using Sentinel-1 time series at field scale, *Remote Sensing,* 2018, 10, 1495; doi:10.3390/rs10091495
- Hajnsek I., Pottier E., Cloude S., «Inversion of surface parameters from polarimetric SAR», *IEEE Transactions on Geoscience and Remote Sensing,* 41(4), p. 727–744, 2003.
- Hallikaïnen M.T., Ulaby F.T., Dobson F.T., El Rayes M.C., Wu L.K., «Microwave dielectric behavior of wet soil. Part I: Empirical models and experimental observations», *IEEE Transactions on Geoscience and Remote Sensing*, 23, p. 25-34, 1985.
- Lasne Y., Paillou P., Freeman A., Farr T., McDonald K.C.,, Ruffié G., Malézieux J.M., Chapman B., Demontoux F., «Effect of salinity on the dielectric properties of geological materials: Implication for Soil Moisture detection by means of radar remote sensing», IEEE Transactions on Geoscience and Remote Sensing, 46(6), p. 1674-1688, 2008.

- Le Hégarat-Mascle S., Zribi, M., Alem, F., Weisse, A., Loumagne C., «Soil moisture estimation from ERS/SAR data: Toward an operational methodology», *IEEE Transactions on Geoscience and Remote Sensing*, 40(12), p. 2647-2658, 2002.
- Le Toan T., «Active microwave signatures of soil and crops- Significant results of three years of experiments», *Proceeding of the International Geoscience and Remote Sensing Symposium, IGARSS 82*, Munich, Germany, 1–4 June 1982 (p. 25–32). New York : IEEE, 1982.
- Lievens H., Vernieuwe H., Alvarez-Mozos J., De Baets B., Verhoest N., «Error in radar-derived soil moisture due to roughness parameterization: an analysis based on synthetical surface profiles», *Sensors Journal,* 9, p. 1067-1093, 2009.
- Oh Y., Sarabandi K., Ulaby F.T., «An empirical model and an inversion technique for radar scattering from bare soil surfaces», *IEEE Transactions on Geoscience and Remote Sensing*, 30(2), p. 370-381, 1992.
- Oh Y., Kay Y., «Condition for precise measurement of soil surface roughness», *IEEE Transactions on Geoscience and Remote Sensing,* 36(2), p. 691-695, 1998.
- Oh Y., Sarabandi K., Ulaby F.T., «Semi-empirical model of the ensemble-averaged differential Mueller matrix for microwave backscattering from bare soil surfaces», *IEEE Transactions on Geoscience and Remote Sensing*, 40, p. 1348–1355, 2002.

- Oh Y., «Quantitative retrieval of soil moisture content and surface roughness from multipolarized radar observations of bare soil surfaces», *IEEE Transactions on Geoscience and Remote Sensing*, 42, p. 596-601, 2004.
- Paloscia S., Pampaloni P., Pettinato S., Santi E., «A comparison of algorithms for retrieving soil moisture from ENVISAT/ASAR images», *IEEE Transactions on Geoscience and Remote Sensing*, 46, p. 3274-3284, 2008.
- Paloscia S., Pettinato S., Santi E., Notarnicola C., Pasolli L., Reppucci A., «Soil moisture mapping using Sentinel-1 images: Algorithm and preliminary validation», *Remote Sensing of Environment*, 134, p. 234-248, 2013.
- Topp G.C., Davis J.L., Annan A.P., «Electromagnetic determination of soil water content: Measurement in coaxial transmission lines», *Water Resources Research*, 16, p. 547-582, 1980.
- Ulaby F.T., Batlivala P.B., Dobson M.C., «Microwave backscatter dependence on surface roughness, soil moisture and soil texture: Part I – Bare soil», *IEEE Transactions on Geoscience and Remote Sensing*, 16, p. 286–295, 1978.
- Ulaby F.T., Moore R.K., Fung A.K., 1986. *Microwave Remote Sensing Active and Passive*. Norwood: Artech House, inc, 1986.
- Verhoest N.E.C., Lievens H., Wagner W., Alvarez-Mozos J., Moran, M.S., Mattia F., «On the soil roughness parameterization problem in soil moisture retrieval of bare surfaces from Synthetic Aperture Radar», *Sensors*, 8(7), p. 4213–4248, 2008.
- Wagner W., Lemoine G., Rott H., «A method for Estimating Soil Moisture from ERS Scatterometer and Soil Data», *Remote Sensing of Environment*, 70, p. 191–207, 1999.

- ZRIBI M., «Développement de nouvelles méthodes de modélisation de la rugosité pour la rétrodiffusion hyperfréquence de la surface du sol», Thèse de Doctorat, Université de Toulouse, France, 1998.
- ZRIBI M., CIARLETTI V., TACONET O., «Validation of a rough surface model based on fractional brownian geometry with SIRC and ERASME radar data over Orgeval site», *Remote Sensing of Environment*, 73, p. 65-72, 2000.
- ZRIBI, M., CIARLETTI, V., TACONET, O., VIDAL-MADJAR, D., «Effect of rows structure on radar microwave measurements over soil surface», *International Journal of Remote Sensing*, 23(24), p. 5211-5224, 2002.
- ZRIBI M., DECHAMBRE M., «An new empirical model to retrieve soil moisture and roughness from Radar Data», *Remote Sensing of Environment*, 84, p. 42-52, 2003.
- ZRIBI M., BAGHDADI N., HOLAH N., FAFIN O., «New methodology for soil surface moisture estimation and its application to ENVISAT-ASAR multi-incidence data inversion», *Remote Sensing of Environment,* 96, p. 485-496, 2005.
- ZRIBI, M., SAUX-PICART, S., ANDRÉ, C., DESCROIX, L., OTTLÉ, O., KALLEL, A., «Soil moisture mapping based on ARSAR/ENVISAT radar data over a sahelian site», *International Journal of remote Sensing*, 28(16), p. 3547-3565, 2007.

- Zribi, M., Chahbi, A., Lili, Z., Duchemin, B., Baghdadi, N., Amri, R., Chehbouni, A., «Soil surface moisture estimation over a semi-arid region using ENVISAT ASAR radar data for soil evaporation evaluation», *Hydrology and Earth System Sciences,* 15, p. 345-358, 2011.
- Zribi, M., Kotti, F., Lili-Chabaane, Z., Baghdadi, N., «Soil texture mapping over a semi-arid area using TERRASAR-X radar data over a semi-arid area», *IEEE Transactions on Geoscience and Remote Sensing Letters*, 9(3), p. 353-357, 2012.
- Zribi M., Baghdadi N., Le Hégarat S., Ottlé C., Loumagne C., «Suivi de l'état hydrique du sol par télédétection radar», Editeurs Loumagne C. et Tallec G., L'observation long terme en environnement, Exemple du bassin de l'Orgeval, éditions QUAE, Versailles, 2013.
- Zribi M., Gorrab A., Baghdadi N., «A new soil roughness parameter for the modelling of radar backscattering over bare soil», *Remote Sensing of Environment*, 152, p. 62-73, doi:10.1016/j.rse.2014.05.009, 2014.
- Zribi M., Gorrab A., Baghdadi N., Lili-Chabaane Z., «Influence of radar frequency on the relationship between bare surface soil moisture vertical profile and radar backscatter», *IEEE Geoscience and Remote Sensing Letters,* 11(4), p. 848-852
- Zribi M., Sahnoun M., Baghdadi N., Le Toan T., Ben Hamida A., 2016. Analysis of the relationship between backscattered P-band radar signals and soil roughness. *Remote Sensing of Environment*, vol. 8, pp. 13-21
- Zribi M., Muddu S., Bousbih S., Al Bitar A., Tomer S.K., Baghdadi N., Bandyopadhyay S., 2019. Analysis of L-band SAR data for soil moisture estimations over agricultural areas in the tropics. Remote Sensing, 2019, 11, 1122, doi:10.3390/rs11091122, 22 pages

- El Hajj M., Baghdadi N., Zribi M., 2018. Estimation de l'humidité du sol par couplage d'images radar et optique. Chapitre book: Baghdadi N., Mallet C., et Zribi M. (eds), QGIS et applications en agriculture et forêt, vol. 2, p. 15-58, 2018, ISTE Editions, 374 pp.
- El Hajj M., Baghdadi N., Zribi M., 2018. Coupling radar and optical data for soil moisture retrieval over agricultural areas. Chapter book: Baghdadi N., Mallet C., and Zribi M. (eds), QGIS and applications in Agriculture and Forest, vol. 2, p. 1-46, 2018, ISTE-Wiley Editions, 364 pp.
- El Hajj M., Zribi M., Baghdadi N., Lepage M., 2018. Cartographie de la sécheresse. Chapitre book: Baghdadi N., Mallet C., et Zribi M. (eds), QGIS et applications en eau et risques, vol. 4, p. 209-240, 2018, ISTE Editions, 320 pp.
- El Hajj M., Zribi M., Baghdadi N., Lepage M., 2018. Mapping of Drought. Chapter book: Baghdadi N., Mallet C., and Zribi M. (eds), QGIS and applications in water and risks, vol. 4, p. 185-214, 2018, ISTE-Wiley Editions, Wiley, 306 pp.
- Baghdadi N., Zribi M., 2016. Characterisation of soil surface properties using radar remote sensing. Chapitre book: Baghdadi N. and Zribi M. (eds), *Land surface remote sensing in continental hydrology*, p. 1-40, Septembre 2016, Elsevier, 502 pp.

- Baghdadi N., et Zribi M., 2016. Caractérisation des états de surfaces des sols par télédétection radar. Chapitre book: Baghdadi N. et Zribi M. (eds), *Observation des Surfaces Continentales par Télédétection: Hydrologie continentale*, vol. 4, p. 21-54, 2016, ISTE Editeur, Elsevier, 456 pp.
- Zribi M. and Baghdadi N., 2015. Potential of high spatial resolution radars for the characterization of soil propertiesin agricultural environments. Chapitre book: Lucke, B., Bäumler, R., Schmidt, M. (eds), Soils and Sediments as Archives of landscape change in the subtropics and tropics. Erlanger Geographische Arbeiten Band, ISBN 978-3-941665-04-0, 42, Chapter 4, pp. 33–52.
- Zribi M., Baghdadi N., Le-Hégarat S., and Loumagne C., 2013. Suivi de l'état hydrique du sol par télédétection radar. Chapitre ouvrage QUAE « L'observation long terme pour la recherche en environnement, exemple du Bassin Versant de l'Orgeval (1962-2012) », Editions QUAE, ISBN : 978-2-7592-2073-1, pp. 257-268.
- Baghdadi N., Zribi M., Aubert M., and Loumagne C., 2013. Performance des capteurs radar à synthèse d'ouverture pour la caractérisation des états de surface des sols en milieux agricoles. Chapitre ouvrage QUAE « L'observation long terme pour la recherche en environnement, exemple du Bassin Versant de l'Orgeval (1962-2012) », Editions QUAE, ISBN : 978-2-7592-2073-1, pp. 231-243.

TETIS

iSTE editions

Série de 6 volumes coordonnée par
André Mariotti, Université Pierre et Marie Curie
SYSTEME TERRE – ENVIRONNEMENT

Télédétection pour l'observation des surfaces continentales

série de 6 volumes sous la direction de

Nicolas Baghdadi, IRSTEA Montpellier
et Mehrez Zribi, CESBIO Toulouse

L'utilisation de la télédétection pour observer notre environnement a fondamentalement révolutionné la façon dont nous modélisons les processus et systèmes environnementaux. Cette série regroupe les travaux de près de 200 chercheurs de renommée internationale en six volumes pour nous présenter une « boîte à outils » complète des méthodes et actions scientifiques les plus modernes en terme d'utilisation de l'observation spatiale.

Les deux premiers volumes décrivent les principes physiques des différentes techniques couvrant le spectre des fréquences. Le troisième volume illustre des applications de l'observation spatiale destinées à l'agriculture et la forêt. Le volume quatre présente des applications de l'observation spatiale en hydrologie. Le cinquième volume est dédié à l'observation des zones urbaines et côtières, et le dernier volume présente l'application de l'observation spatiale à la compréhension et à l'évaluation des risques.

DÉTAIL DES VOLUMES DE LA SÉRIE

Volume 1 *(352 pages – 70,00 € – ISBN 9781784051563)*
Observation des surfaces continentales par télédétection optique : techniques et méthodes

Volume 2 *(408 pages – 85,00 € – ISBN 9781784051570)*
Observation des surfaces continentales par télédétection micro-onde : techniques et méthodes

Volume 3 *(368 pages – 95,00 € – ISBN 9781784051587)*
Observation des surfaces continentales par télédétection : agriculture et forêt

Volume 4 *(456 pages – 90,00 € – ISBN 9781784051594)*
Observation des surfaces continentales par télédétection : hydrologie continentale

Volume 5 *(364 pages – 70,00 € – ISBN 9781784051600)*
Observation des surfaces continentales par télédétection : urbain et zones côtières

Volume 6 *(360 pages – 70,00 € – ISBN 9781784051617)*
Observation des surfaces continentales par télédétection : environnement et risques

Tous les titres de la série seront disponibles fin novembre 2016 auprès de votre libraire ou d'Amazon.fr

iSTE

An important publication coordinated by
André Mariotti, Université Pierre et Marie Curie, France
EARTH SYSTEM – ENVIRONNEMENT

Remote Sensing Observations of Continental Surfaces

A 6 volumes set edited by

Nicolas Baghdadi, IRSTEA Montpellier
et Mehrez Zribi, CESBIO Toulouse, France

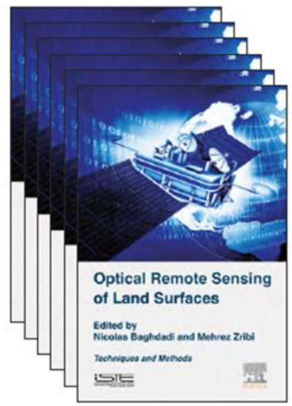

Remote sensing observations is one of the key disciplines that allow the analysis and provide access to the understanding of the functioning of our environment.

This Set mobilized almost 200 internationally recognized researchers to propose a comprehensive "toolkit", describing the latest scientific methods and actions in terms of the implementation of spatial observation.

The first two volumes describe the physical principles underlying various techniques which cover the frequency spectrum ranging from visible to microwaves.

The third volume illustrates the agricultural and forestry applications of spatial observation.

The fourth volume presents the applications of spatial observation in the field of continental hydrology.

The fifth volume is dedicated to the observation of urban and coastal areas, whereas the final volume presents the implementation of spatial observation within the context of risk assessment and understanding.

The volumes

Optical Remote Sensing of Land Surfaces
Techniques and Methods
ISBN 9781785481024 • 2016 • 388 pages

Microwave Remote Sensing of Land Surfaces
Techniques and Methods
ISBN 9781785481598 • 2016 • 448 pages

Land Surface Remote Sensing in Agriculture and Forest
ISBN 9781785481031 • 2016 • 496 pages

Land Surface Remote Sensing in Continental Hydrology
ISBN 9781785481048 • 2016 • 502 pages

Land Surface Remote Sensing in Urban and Coastal Areas
ISBN 9781785481604 • 2016 • 392 pages

Land Surface Remote Sensing
Environment and Risk
ISBN 9781785481055 • 2016 • 384 pages

About the Authors

Nicolas Baghdadi is Research Director at IRSTEA in France. He is currently the scientific director of the French Land Data Centre (Theia).

Mehrez Zribi is Research Director at CNRS in France. He is currently active at CESBIO in Toulouse where he is also responsible for the team of observation systems.

The 6 volumes of this Set are published by ISTE-Elsevier • Ordrer: http://store.elsevier.com

iSTE editions

LEADER DE L'EDITION FRANCAIS D'OUVRAGES EN SCIENCES ET TECHNIQUES

Série Utilisation de QGIS en télédétection

coordonnée par André Mariotti

sous la direction de Nicolas Baghdadi, Clément Mallet et Mehrez Zribi

La série *Utilisation de QGIS en télédétection* vise à faciliter l'appropriation et l'utilisation opérationnelle du système d'information géographique (SIG) QGIS (Quantum Geographie Information System) dans le domaine de la télédétection.

QGIS et outils génériques
Volume 1 • 316 pages • Ouvrage papier 978-1-78405-335-2 : 70,00 €
Ce volume définit le principe de fonctionnement de QGIS et des librairies fondamentales les plus fréquemment utilisées en traitement d'images et en géomatique.

QGIS et applications en agriculture et forêt
Volume 2 • 374 pages • Ouvrage papier 978-1-78405-336-9 : 84,00 €
QGIS et applications en agriculture et forêt présente différents exemples en agriculture et en foresterie.

QGIS et applications en aménagement du territoire
Volume 3 • 306 pages • Ouvrage papier 978-1-78405-337-6 : 70 ,00 €
Ce troisième volume retrace la mise en pratique sous QGIS et ses librairies de différentes applications en lien avec l'aménagement du territoire.

QGIS et applications en eau et risques
Volume 4 • 320 pages • Ouvrage papier 978-1-78405-338-3 : 70,00 €
Ce quatrième volume de la série expose la présentation et la mise en pratique sous QGIS et ses librairies des applications traitant des problématiques eau et risques.

Le format ebook est à 9,90 €
(Offre uniquement pour les particuliers disponible sur iste-editions.fr)

SET

QGIS in Remote Sensing

Coordinator: André Mariotti, UPMC, Paris, France

The QGIS in Remote Sensing Set aims to facilitate the appropriation and operational use of the Quantum Geographic Information System (QGIS) software in the field of remote sensing.

VOLUME 1 – QGIS AND GENERIC TOOLS

Edited by Nicolas Baghdadi, IRSTEA, Clément Mallet, INIGF, Mehrez Zribi, CNRS, France

This first volume describes the operating principles of QGIS and the most frequently used and fundamental libraries in image processing and geomatics: GDAL, GRASS, SAGA and OTB. It presents many core features that will be implemented in various practical cases of remote sensing and spatial analysis in the other three volumes of the set.

VOLUME 2 – QGIS AND APPLICATIONS IN AGRICULTURE AND FOREST

Edited by Nicolas Baghdadi, IRSTEA, Clément Mallet, INIGF, Mehrez Zribi, CNRS, France

This second volume of the set presents different applications of QGIS and its libraries for agriculture and forestry. A thorough knowledge of agriculture and forest areas is fundamental from both an economic and an environmental point of view. These environments are strongly involved in the use of spatial data, which are essential for restoring the spatio-temporal variability of surface conditions. In this context, GIS tools have long been used to support the exploitation of spatial imagery.

VOLUME 3 – QGIS AND APPLICATIONS IN TERRITORIAL PLANNING

Edited by Nicolas Baghdadi, IRSTEA, Clément Mallet, INIGF, Mehrez Zribi, CNRS, France

Over the past 15 years, Geographic Information Systems have become central to applications dealing with territorial planning issues. This third volume of the set is devoted to the presentation and practice in QGIS and its libraries of various applications related to territorial planning. The chapters illustrate the great diversity of case studies, spatial scales and actors involved in this issue: from the world to the city and from objects of special interest, from detection of objects, to studies of location or the impact of works through spatial indicators, urban, agro-forestry or coastal environments.

VOLUME 4 – QGIS AND APPLICATIONS IN WATER AND RISKS

Edited by Nicolas Baghdadi, IRSTEA, Clément Mallet, INIGF, Mehrez Zribi, CNRS, France

This fourth volume of the set is dedicated to the presentation and the practice of QGIS and its libraries of applications dealing with water and risk management issues. In the context of global changes (climatic and anthropogenic), understanding and quantifying water resource dynamics and the various aspects of risks is essential for managers in public authorities and local population.